

2009-01-01

Analysis of EMG During Clonus Using Wavelets

Chaithanya Krishna Mummidisetty
University of Miami, c.mummidisetty@miami.edu

Follow this and additional works at: https://scholarlyrepository.miami.edu/oa_theses

Recommended Citation

Mummidisetty, Chaithanya Krishna, "Analysis of EMG During Clonus Using Wavelets" (2009). *Open Access Theses*. 41.
https://scholarlyrepository.miami.edu/oa_theses/41

This Open access is brought to you for free and open access by the Electronic Theses and Dissertations at Scholarly Repository. It has been accepted for inclusion in Open Access Theses by an authorized administrator of Scholarly Repository. For more information, please contact repository.library@miami.edu.

UNIVERSITY OF MIAMI

ANALYSIS OF EMG DURING CLONUS USING WAVELETS

By

Chaithanya Krishna Mummidisetty

A THESIS

Submitted to the Faculty
of the University of Miami
in partial fulfillment of the requirements for
the degree of Master of Science

Coral Gables, Florida

May 2009

©2009

Chaithanya Krishna MummidiSetty

All Rights Reserved

UNIVERSITY OF MIAMI

A thesis submitted in partial fulfillment of
the requirements for the degree of
Master of Science

ANALYSIS OF EMG DURING CLONUS USING WAVELETS

Chaithanya Krishna Mummidisetty

Approved:

Jorge Bohorquez, Ph.D.
Research Assistant Professor of
Biomedical Engineering

Terri A. Scandura, Ph.D.
Dean of the Graduate School

Christine K. Thomas, Ph.D.
Professor of Neurological
Surgery

Weizhao Zhao, Ph.D.
Associate Professor of
Biomedical Engineering

MUMMIDISSETTY, CHAITHANYA KRISHNA

(M.S., Biomedical Engineering)

Analysis of EMG During Clonus Using Wavelets

(May 2009)

Abstract of a thesis at the University of Miami.

Thesis supervised by Dr. Jorge Bohorquez and Dr. Christine K. Thomas.

No. of pages in text. (92)

Involuntary muscle contractions (spasms) are a major secondary consequence of spinal cord injury. These spasms disrupt mobility and the ability to perform daily activities. The rhythmic repetitive muscle contractions of clonus are one kind of spasm. In this study an algorithm was developed to automatically detect the start and end times of EMG bursts during clonus. These measures were used to calculate the duration of EMG bursts, clonus frequency and the intensity (root mean square) of each EMG burst, parameters that characterize clonus.

This algorithm relied on the technique of intensity analysis (Von Tscherner 2000). Filters were created by non-linearly scaling a Mother (Morlet) wavelet to produce envelopes of the EMG in different frequency bands. The intermediate frequency band (80-190 Hz) enveloped the EMG best and was used to detect the EMG bursts during clonus. To detect the EMG bursts, an intensity threshold and time separation threshold were imposed on the algorithm to eliminate multiple peaks caused by the baseline EMG, motor units or EMG changes. Window regions were extended between the midpoints of identified EMG peaks then resized to 50 ms on either side of each identified EMG peak. The start and end times of EMG bursts were at 5% and 95% of the energy contained in a window region, respectively. A motor unit threshold constraint was used to eliminate

motor unit potentials at the beginning and end of clonus. The algorithm output from 31 spasms in long term (24 hr) EMG data recorded from 8 paralyzed leg muscles of 7 subjects with a chronic cervical spinal cord injury were compared to that generated by two independent human operators. The algorithm was as good as a human operator at identifying EMG bursts ($p = 0.946$), clonus frequency (intra class correlation coefficient $\alpha = 0.949$), contraction intensity ($\alpha = 0.997$) and the durations of each burst of EMG during clonus ($\alpha = 0.852$). On average the algorithm was 574 (SE 238) times faster than manual analysis by two people ($p \leq 0.001$). Analysis of clonus in one 24 hour dataset from the right medial gastrocnemius muscle with the algorithm showed that clonus was more prevalent and stronger during awake versus sleep time. This algorithm can be used to analyze long term recordings accurately with limited user intervention. The algorithm may also be a prospective diagnostic tool to judge the effectiveness of interventions such as drugs like baclofen that are used to mitigate clonus.

This is dedicated to my parents and family

Acknowledgements

I would like to thank Dr. Christine K. Thomas for her guidance and motivation to accomplish this dream project. I had to go back to the drawing board several times to improve efficiency of the methods developed. It was Dr. Chris who taught me lessons of perfection, which I will cherish for the rest of my life.

I would also like to thank Dr. Jorge Bohorquez for his advice and guidance in developing this project. His vision and approach chiseled my problem-solving abilities. I really appreciate your support and encouragement during my career at the University of Miami.

I would like to extend my gratitude to the members of Dr. Thomas Lab for their encouragement and critical review on my work.

Finally I wish to express my love and respect to my parents for their motivation and support in pursuing this endeavor.

TABLE OF CONTENTS

		Page
LIST OF FIGURES		viii
LIST OF TABLES		xii
 Chapter		
1	INTRODUCTION	1
2	OBJECTIVES	3
3	BACKGROUND	5
	3.1 Anatomy of the spinal cord	5
	3.2 Spinal cord injury classification.....	5
	3.3 Muscle properties after SCI	6
	3.4 Stretch reflex pathway	8
	3.5 Spasticity, Spasms and clonus	9
	3.5.1 Mechanisms underlying clonus.....	10
	3.5.2 Evidence to support different mechanisms of clonus	11
	3.5.3 Motor unit behavior during clonus	14
	3.6 Clonus summary	15
	3.7 Analysis of EMG	15
4	METHODS	17
	4.1 Data collection and processing	17
	4.1.1 Muscles and electrode configuration	18
	4.1.2 Logger setup.....	19
	4.1.3 Calibration.....	21

4.1.4	Stimulation protocol.....	21
4.1.5	24 hour EMG recording.....	22
4.1.6	EMG processing.....	22
4.2	Algorithm to detect onset and offset of each EMG burst during	
	Clonus	24
4.2.1	Creation of bank of filters using Morlet wavelet.....	26
4.2.2	Intensity analysis to envelope EMG.....	28
4.2.3	EMG burst detection.....	32
4.2.4	Marking onset and offset of EMG bursts.....	35
4.2.5	Calculation of clonus parameters.....	39
4.3	Manual measurements	41
4.4	Visual comparison of measurements	44
4.5	Comparison of outputs from the algorithm and human operators.....	46
4.5.1	Template structure and organization.....	46
4.5.2	Data transfer to excel template	46
4.6	Automatic clonus analysis by the algorithm.....	48
4.6.1	Single clonus analysis.....	48
4.6.2	Analysis of clonus in 24 hour recordings	48
4.7	Statistics	49
5	RESULTS	51
5.1	Performance evaluation	51
5.1.1	Number of common bursts of EMG	51
5.1.2	Start and end time difference	53
5.1.3	Discrepancies in start and end times.....	57
5.1.4	On duration	59
5.1.5	Clonus frequency	62
5.1.6	Intensity of contractions.....	68

5.1.7	Measurement time.....	72
5.2	Analysis of clonus in single muscle over 24 hours.....	72
5.2.1	Number of EMG bursts during clonus.....	73
5.2.2	On duration.....	75
5.2.3	Clonus frequency	76
5.2.4	Intensity of contractions.....	77
5.2.5	Changes in parameters during clonus	79
6	DISCUSSION	82
6.1	Detection of bursts of EMG during clonus.....	82
6.2	Measurement of the start and end of the EMG burst.....	83
6.3	Analysis time	86
6.4	Characterization of clonus	86
6.5	Limitations and future developments.....	87
7	CONCLUSIONS.....	89
	REFERENCES	90

LIST OF FIGURES

	Page
Fig. 3.1 Stretch reflex pathway	9
Fig. 4.1 Electrode configuration employed for the four leg muscles.....	19
Fig. 4.2 Equipment for recording 24 hour EMG	20
Fig. 4.3 Example of manually marked start and end of EMG bursts during clonus....	24
Fig. 4.4 Flow chart of detection algorithm	25
Fig. 4.5 Filter bank of wavelets	28
Fig. 4.6 User interface to view intensity envelopes and EMG	30
Fig. 4.7 Linear envelopes to EMG.....	31
Fig. 4.8 Number of peaks identified by algorithm with changing time constraint	34
Fig. 4.9 Example of peaks detected in envelope to EMG during clonus.....	34
Fig. 4.10 Detection windows to detect start and end of EMG burst.....	37
Fig. 4.11 Example of EMG during clonus along with motor units and tonic burst.....	39
Fig. 4.12 User interface to select data for making manual measurements	42
Fig. 4.13 Dadisp window to view and mark start and end times of EMG bursts	42
Fig. 4.14 User interface to select data to make visual comparisons	44

Fig. 4.15	Display output produced by user interface to make visual comparisons	45
Fig. 4.16	User interface to analyze clonus and transfer outputs to excel template.....	47
Fig. 5.1	Percentage agreement on number of common bursts.....	52
Fig. 5.2	Example of start and end time differences between operators and program..	54
Fig. 5.3	Histograms for the start time differences between Person 1 and Person 2.....	55
Fig. 5.4	Histograms of average start time differences between operators and the program	56
Fig. 5.5	Histograms of average end time differences between operators and the program	56
Fig. 5.6	Average contributions of discrepancies in measuring start and end times.....	58
Fig. 5.7	Example of duration of EMG bursts measured by operators and the program	59
Fig. 5.8	Example for percentage agreement on on durations between operators and the program60
Fig. 5.9	Mean agreement for on duration measured by operators and the program	61
Fig. 5.10	Mean distribution of percentage agreement for on duration between operators and Person1 and the program.....	62
Fig. 5.11	Example of clonus frequency measured by operators and the program.....	63

Fig. 5.12	Mean agreement on clonus frequency measured by operators and the program	64
Fig. 5.13	Average percentage difference in clonus frequency measured by operators and the program	65
Fig. 5.14	Number of EMG bursts identified without constraints and with addition of each set of constraints	66
Fig. 5.15	EMG bursts detected by the algorithm compared to Person 1	67
Fig. 5.16	Mean agreement on the number of peaks identified by the Person 1 and the program	68
Fig. 5.17	Example of RMS values of EMG bursts measured by operators and the program	69
Fig. 5.18	Average agreement on RMS value of EMG bursts between operators and Person1 and the program.....	70
Fig. 5.19	Average percentage difference in RMS values of EMG bursts measured by operators and the program	71
Fig. 5.20	Example of average number of EMG bursts during clonus in 24 hours	74
Fig. 5.21	Mean EMG burst durations during clonus in 24 hours	75
Fig. 5.22	Mean clonus frequencies during 24 hours.....	76
Fig. 5.23	Average RMS EMG of bursts during clonus in 24 hours.....	78

Fig. 5.24	Average duration of EMG bursts during clonus presented independent of clonus duration	79
Fig. 5.25	Average clonus frequency presented independent of clonus duration 24 hours.....	80
Fig. 5.26	Average RMS EMG of bursts during clonus presented independent of Clonus duration.....	81

LIST OF TABLES

	Page
Table. 4.1 Subject history	17
Table. 4.2 Central frequencies	27

Chapter 1: Introduction

Spinal cord injury (SCI) usually results in paralysis of skeletal muscles innervated from the spinal segments below the level of the lesion. Although not under voluntary control, these muscles start to contract involuntarily after a few weeks. These involuntary muscle contractions (spasms) can be associated with hyperactive reflexes and increases in muscle tone, all symptoms of spasticity and a major secondary consequence of spinal cord injury.

One kind of spasm is clonus. Clonus is characterized by rhythmic involuntary muscle contractions. The severity of clonus has been reported to vary from mild to extremely distracting. These contractions interfere with mobility and the ability to perform basic activities. To understand clonus, a few studies have recorded electromyographic signals during clonus in a laboratory setting. Whether these data provide a representative picture of the daily clonus occurring in SCI subjects is unclear. The average frequency of the contractions has been measured during the steady state period of the clonus (Walsh 1976, Dimitrijevic et al. 1980, Iansek 1984, Rack et al. 1984, Rossi et al. 1990, Jones et al. 2003) but not from the beginning to the end of the spasm. The magnitude of the bursts of electromyographic activity (EMG) during clonus has not been evaluated but this could provide valuable information about the severity of the muscle contractions. Some studies have recorded EMG from multiple muscles for brief periods. Moreover, we do not know how common clonus is.

In the present study, clonus will be analyzed in long term EMG recordings (24 hrs) from multiple leg muscles (n=8) that have been paralyzed chronically by spinal cord injury. Data collected over an entire day will provide a more realistic picture of clonus in a natural setting. A complete analysis of the EMG during the entire spasm will reveal how the EMG durations, clonus frequency, and the magnitude of activity changes over time during clonus. Measuring all of these parameters manually is laborious and time consuming, particularly on 24 hr records. Thus, the overall aim of this project is develop an algorithm to automate these analyses, methods that do not exist.

The outcomes of this study are important in terms of understanding involuntary muscle contractions. For example, parameters like the overall duration of clonus can be monitored before and after use of medication like baclofen to judge the efficiency of this treatment.

Chapter 2: Objectives

The long-term objective of this project is to develop an algorithm that automatically marks the start and end of each burst of EMG during clonus in long-term (24 hrs) EMG recordings from people with chronic cervical SCI.

The Specific aims are:

1. To determine the start and end of each burst of EMG in the data manually labeled as clonus.
2. To use the timing of these events to calculate the burst durations (On durations), the instantaneous frequency of contractions during clonus and the RMS (root mean square) value of the EMG during each burst of EMG during clonus.
3. To develop user interfaces in MATLAB and DaDisp to analyze clonus manually so the results of the program can be compared with the outcomes of two different human operators.

Hypotheses

1. Automatic analysis of clonus by the algorithm is as reliable as the manual performance of two people with respect to the EMG burst durations, the frequency of clonus, and the intensity of contractions during clonus.
2. Automatic analysis of clonus by the algorithm is faster than manual analysis by a human operator.

The first hypothesis will be tested by comparing the algorithm outputs with that of two human operators by examining the reliability of intra-class correlations. The second hypothesis will be tested by comparing the total amount of time required for human operators to manually mark the events during clonus and the time taken by the algorithm to perform the same task.

Chapter 3: Background

3.1 Anatomy of the spinal cord

The spinal cord is a crucial part of the central nervous system in humans extending from brain to the lower back (coccyx). It is protected by a column of 33 bones (vertebrae). These vertebrae are divided into 5 sections namely cervical (vertebrae; n = 7), thoracic (n = 12), lumbar (n = 5), sacral (n = 5) and coccyx (n = 4) depending on their location. Ventral and dorsal roots exit these vertebrae and are named according to their origin in the spinal column. The spinal segments and roots are indicated by letters and numbers and are used to reference lesions of the spinal cord. For example C6 indicates the 6th cervical segment.

3.2 Spinal cord injury classification

The spinal cord links the brain and the body by signaling both motor and sensory information to coordinate activities of living. Any lesion to this conduit may result in disruption of motor and/or sensory information from brain to periphery and vice versa. The body functions that are compromised or disrupted depend on the segment of the cord that is injured, and the severity of the injury. As a sequel to this traumatic injury a wide spectrum of consequences are encountered. For example, there is usually muscle paralysis and then involuntary muscle contractions. Respiratory problems, an irregular heartbeat, low blood pressure, loss of bladder, bowel and temperature control, reproductive and sexual functions are also common.

Loss or damage to motor and/or sensory areas in the cervical segments of the spinal cord results in impairment of arm, trunk and leg muscle function. Since all four limbs are influenced, the condition is termed tetraplegia or quadriplegia. All of the participants in this study had cervical lesions.

In order to determine the level and the completeness of injury, sensory and motor functions are evaluated separately but overall both scores are used (Maynard et al. 1997). Sensory function is assessed for each dermatome and is rated on a three point scale (0-2) for appreciation of pin prick and light touch. A value of 0 indicates absence of sensitivity to pin prick and light touch, 1 represents partial or altered appreciation, and a score of 2 is given for normal sensation. Motor function is rated on a six point scale (0-5) for key muscles on either side of the body. A value of 0 represents total paralysis of the muscle, 1 indicates a palpable or visible contraction, 2 indicates the capability for active movement, and full range of motion (ROM) in a gravity eliminated position, 3 represents active movement, full ROM against gravity, 4 is given for active movement, full ROM against moderate resistance and 5 is normal active movement, full ROM against strong resistance.

In this study, all of the lesions were complete which implies that no sensory or motor function was preserved in sacral segments S4-S5.

3.3 Muscle properties after SCI

In addition to the trauma caused by the spinal cord injury itself, several adaptations occur in the neuromuscular system. For example there are changes in muscle

fiber type composition, fiber size, force, speed and fatigue. A description of these changes in muscle properties in response to spinal cord injury is given in this section.

Fiber type composition Human muscles usually have a mix of slow and fast twitch fibers except for muscles like soleus which has a dominance of slow fibers (Grimby et al. 1976). However, with time after spinal cord injury, there is a greater proportion of type II fibers (fast twitch fibers) in almost all skeletal muscles including a postural muscle like soleus, as confirmed by histochemical studies (Grimby et al. 1976, Shields 1995).

Fiber atrophy The fiber diameter of both type I and type II fibers is reduced with time after chronic muscle paralysis compared to that in able bodied subjects (Grimby et al. 1976). Wide spread muscle atrophy is commonly observed after SCI due to altered use of muscle. Atrophy may also reflect chronic denervation of muscle due to motorneuron death from spinal cord injury (Thomas 1997). Denervation leads to decreased fiber diameter of both type I and II fibers and eventually degeneration (Grimby et al. 1976).

EMG and force At the motor unit level there are increases in EMG latencies and durations, and reductions in axon conduction velocities, force and fatigue resistance (Häger-Ross et al. 2006, Klein et al. 2006). Reductions in the amplitude and area of compound muscle action potentials (M-waves; the response to a supra-maximal stimulus to the nerve innervating a target muscle) occur in the paralyzed muscles compared to that measured from muscles of uninjured subjects, which is consistent with the general weakness of paralyzed muscles (Shields 1995, Thomas 1997, Gerrits et al. 1999). The

maximal rate of force rise was 50% faster than in muscles of control subjects suggesting an increase in the contraction speed of paralyzed muscle (Gerrits et al. 1999). However in certain cases, force and contractile speeds were reduced or remained unchanged even after 23 years of SCI (Thomas 1997).

Fatigability Another major consequence of SCI is increased fatigability of paralyzed muscles, identified by an increased loss of force during a sustained contraction. The force generated by different motor units ranged from 8-60% of the initial (pre-fatigue) value after only 2 minutes (Klein et al. 2006). Similar reductions in force occur in whole muscles (Thomas 1997, Gerrits et al. 1999, Shields 2002,) suggesting that ischemia plays only a small role in the force declines (Thomas and Zijdwind 2006). The disassociation of EMG parameters and force along with significant potentiation of EMG amplitude and area during fatigue (i.e., EMG increases while force decreases) indicates safe neuromuscular junction transmission of the signal (Klein et al. 2006). Thus, the fatigue could be due to either impaired handling of calcium ions (Ca^{2+}), and/or to altered cross bridge kinetics.

3.4 Stretch reflex pathway

When a brief sudden stretch is applied to a joint, the muscle spindles respond by sending afferent discharges along Ia nerve fibers to the spinal cord (Fig. 3.1). These Ia afferent inputs activate the parent motoneurons located in the ventral horn of the spinal cord resulting in contraction of the stretched muscle. There is simultaneous inhibition of the antagonistic muscle(s) via inhibitory interneurons. In healthy individuals the reflex circuitry is under the governance of supraspinal structures. In SCI subjects with complete

lesions, the supraspinal control over reflex pathways below the injury is eliminated. This reduces both the excitation and inhibition of spinal circuitry, which may result in hyperexcitable reflexes.

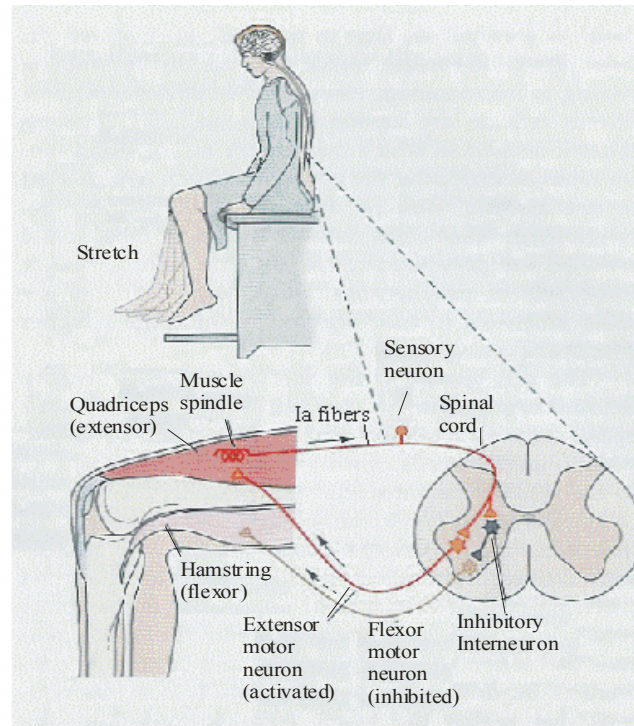


Fig. 3.1. Stretch reflex pathway (modified from Morgenson 1977).

3.5 Spasticity, spasms and clonus

Spasticity is a spectrum of motor disorders characterized by velocity dependent increases in tonic stretch reflexes (Lance 1980), involuntary muscle contractions (muscle spasms) and increased muscle tone (Dietz et al. 1991). Thus spasms are only one of a multitude of disorders that characterize spasticity. One kind of muscle spasm is clonus. Clonus involves bursts of EMG separated by silent periods resulting in rhythmic, repetitive muscle contractions (Walsh 1976, Dimitrijevic et al. 1980, Rack et al. 1984).

This type of abnormal muscular activity commonly occurs secondary to SCI and other neurological impairments that result in interruption of descending motor pathways.

Clonus occurs in leg, arm and hand muscles (Walsh 1976, Ianssek 1984). The severity of clonus varies over a wide range. Contractions have been described as manageable to extremely distracting. Since these contractions are involuntary, they can make it difficult to perform daily activities (Little et al. 1989, Sheean 2002, Adams and Hicks 2005).

How is clonus initiated? Clonus can be initiated by a number of means such as muscle stretch, cutaneous inputs or peripheral nerve stimulation. In a clinical or laboratory setting, clonus is often induced by applying a sudden transient load (or a brief stretch) to the ankle joint resulting in periodic ankle dorsiflexion which may continue as long as a biasing load is maintained (Cook 1967, Walsh 1976, Dimitrijevic 1980, Hidler and Rymer 2000). Other studies have induced clonus by plantar flexion of the ankle joint (Jones et al. 2003), by gently lifting and dropping the knee joint (Wallace et al. 2005), by electrical stimulation of the nerve, or by tapping the tendon (Rossi et al. 1990).

3.5.1 Mechanisms underlying clonus

The mechanisms underlying clonus are controversial. There are two predominant theories to explain clonus. The most popular and widely accepted explanation for clonus is that it involves repetitive stretch reflexes. A brief stretch of a muscle excites Ia afferent fibers. These inputs travel to the spinal cord and excite motoneurons to produce a reflex contraction of the effector muscles. A repetition of this sequence of events is described as a potential reason for the repeated contractions of clonus (Cook 1967, Ianssek 1984, Rack et al. 1984, Hidler and Rymer 2000).

The alternative view point proposes that clonus is primarily dependent on the activity of a central generator within the spinal cord (spinal pacemaker) which rhythmically activates the alpha motoneurons resulting in periodic contractions of the muscles (Walsh 1976, Dimitrijevic et al. 1980). Another group suggests that the interaction of the central pacemaker and peripheral factors may be responsible for clonus. Peripheral events like a tendon tap or a brief muscle stretch may initiate clonus and the regulation of the repeated contractions involves a central generator (Jones et al. 2003). Others suggest that central structures of the nervous system are activated by the peripheral inputs to produce rhythmic contractions, which are often limited to the motoneurons of one or two spinal segments (Wallace et al. 2005).

3.5.2 Evidence to support the different mechanisms of clonus

Reflex mechanisms Evidence that supports a reflex mechanism for clonus includes:

1. Complete block of the common peroneal nerve to ankle flexor muscles does not change the rate and magnitude of clonus in ankle extensors muscles. Thus, clonus can be initiated and sustained in a single muscle group. It does not require alternating stretch reflexes between antagonistic pairs of muscles, suggesting that clonus may be generated and sustained by local afferent inputs and spinal circuitry (Cook 1967).

2. There is a linear inverse relationship between clonus frequency and reflex path length. That is, a longer reflex path results in clonus at a slower frequency. Thus, the timing of the peripheral inputs arriving at the spinal cord can change clonus frequency (Ianssek 1984).

3. In a study on children the muscle twitch durations were shorter, possibly due to fiber type changes in paralyzed muscles allowing them to contract and relax faster. As a result, the muscle contraction, relaxation, and afferent inputs are generated earlier, and when coupled with a shorter path length in children, it is possible to produce the repetitive contractions of clonus at a higher frequency than in adults supporting the reflex mediated theory of clonus (Lin et al. 1999).

4. When a sinusoidal flexion-extension movement at a frequency of 3-7 Hz was imposed on a spastic ankle joint, this assisted the movement rather than resisting the contraction. There was an increase in the magnitude of the EMG but not in the movement frequency, indicating that the high gain of the reflex pathway was responsible for these abnormal reflex responses. The clonus frequency was shown to increase with an increase in the applied mechanical load on the limb supporting the idea that peripheral inputs have effects on clonus frequency (Rack et al. 1984).

5. When a H-reflex was evoked in between two clonic contractions at increasing intervals from the previous contraction there was a progressive shift in the onset of the next contraction indicating that changes in the timing and the amount of the peripheral input can alter EMG onset during clonus. Since the H-reflex is largely considered to be a Ia afferent initiated monosynaptic reflex, these data suggest that clonus involves reflex mediated contractions (Rossi et al. 1990).

6. In a modeling study, Hidler and Rymer (2000) predicted that the oscillatory movements caused during clonus are due to instability in the reflex pathway (feed back loop) forming a stable limit cycle, where peripheral receptors (Ia afferents) make (ankle)

movements both periodic and extremely stable to small perturbations, suggesting that reflex loop nonlinearities are responsible for self-excitation of muscles and the periodic nature of clonus.

Central mechanisms Evidence to support that central mechanisms are responsible for clonus include:

1. In oscillatory systems, the frequency of movements can normally be changed by the appropriate application of a rhythmic signal close to the frequency of the oscillation. That is, clonus should entrain its rhythm to that of the applied frequency if the underlying cause is a reflex mechanism. This result was not observed. Thus clonus was attributed to a spinal generator mechanism (Walsh 1976). This observation is consistent with the data of Rack et al. (1984) and Hidler and Rymer (2000) but the explanation differs.

2. Tapping the tendon of a muscle undergoing clonus did not result in an increase in clonus frequency and it was suggested that a central generator may be responsible for the lack of change in behavior (Dimitrijevic et al. 1980). If a reflex mechanism was responsible for clonus, the tendon tapping should result in an increase in clonus frequency. This did not occur, possibly because the tendon tapping may have resulted in asynchronous activation of the Ia afferents and the inputs may be of insufficient magnitude to excite enough alpha motoneurons to bring about a change in the clonus frequency. Had synchronous stimuli been delivered, such as electrical stimulation of a peripheral nerve at sufficient strength, then the proposed resetting of contraction onset may have been observed (Rossi et al. 1990).

3. Similar clonic EMG activity was observed whether the muscle tendon was stretching or shortening suggesting no role for reflex activity in clonus, hence favoring a central mechanism for clonus (Jones et al. 2003).

3.5.3 Motor unit behavior during clonus

Three different patterns of motor unit activity have been observed during clonus:

1. Units fire one potential in every cycle. The majority of units (98% of recorded data) conform to this firing pattern which suggests that the afferent activity produced by the previous burst of EMG was enough for the motor unit to fire once in every cycle but insufficient to fire at higher rates.

2. A few motor units (1% of recorded data) fired one potential in some cycles but not necessarily in consecutive cycles of clonus. Presumably the afferent activity from the previous contraction was insufficient to excite these motor units in every contraction cycle.

3. The remaining 1% of recorded motor units fired in bursts i.e., more than once per cycle (Wallace et al. 2005).

3.6 Clonus summary

Understanding parameters that characterize clonus is important for both evaluations of possible treatment methods and to judge the treatment in a quantitative way. A number of studies have been carried out on clonus and its underlying mechanisms but only a few studies have focused on quantifying clonus. Earlier studies that have measured clonus frequency have usually only considered the steady state period of clonus, where the contractions appear to be clock-like. The magnitude of the EMG in each contraction has not been evaluated, which could provide valuable information regarding the severity of muscle contractions. Only a few studies have recorded EMG from multiple muscles and for a limited duration in a laboratory setting. This environment may not provide a representative picture of the prevalence of clonus occurring in muscles paralyzed by SCI. Given these unexplored areas, the present study will measure durations of EMG bursts (on durations), clonus frequency and the magnitude of the EMG to quantitatively analyze clonus from the start to the end of the spasm. Analyzing data from long term EMG recordings (24 hrs) from muscles paralyzed by spinal cord injury is important to quantify clonus behavior and its prevalence.

3.7 Analysis of EMG

Conventional analysis of EMG data employs rectification and integration of signals or root mean square values to extract information associated with the amplitude of the signals. This type of analysis deals with the time domain representation of the signal, whereas the frequency content of EMG is typically analyzed using Fourier transforms. In Fourier transforms the temporal (time) aspect of the signal is collapsed. Thus, analysis

with these techniques is uni-dimensional. Analysis that combines both time and frequency can be accomplished by using short-term Fourier transforms (STFTs) and wavelets. With wavelets, the mother wavelet is scaled linearly when the time resolution of events is unknown. Non-linear scaling of wavelets is required when the timing of events in the EMG signals is important. The technique of scaling wavelets non-linearly was developed by Vincent Von Tscharner (2000) and is utilized in the current algorithm developed for analysis of EMG during clonus.

Chapter 4: Methods

4.1 Data collection and processing

The EMG data were collected from 7 subjects (5 male and 2 female, mean age: 39 yr, SE 4, range: 27-52 yr) with a chronic cervical spinal cord injury (mean time since injury: 18 yr (SE 4; range: 4-33 yr, Table 4.1). These injuries were caused by diving mishaps (n=4), motor vehicle accidents (n=2) and sports events (n=1). The injuries were at C4 (n=1), C6 (n=5) or C7 (n=1) and were complete (AISA A) according to American Spinal Injury Association criteria (Maynard et al. 1997). The subjects had no voluntary control of any leg muscles, indicated by an inability to generate any voluntary EMG activity. Subjects took no medication to mitigate muscle spasms. Before participating in the study all subjects gave informed, written consent which was approved by the Institutional Review Board of the University of Miami. One 24-hour recording was performed on each subject.

Table 4.1. Subject history

Subject	Sex	Age (yrs)	Level of injury	Injury duration (yrs)	Cause of injury
A	M	52	C6	33	Diving
B	F	51	C6	25	Motor vehicle accident
C	M	27	C6	4	Diving
D	M	33	C7	14	Motor vehicle accident
E	M	36	C6	11	Diving
F	M	27	C4	10	Diving
G	F	50	C6	30	Sports

4.1.1 Muscles and electrode configuration

Surface EMG signals were recorded simultaneously from 8 leg muscles: vastus lateralis (VL), biceps femoris (HAM), tibialis anterior (TA) and medial gastrocnemius (MG) in each leg. A bipolar configuration was used to record EMG from each muscle. Three new self adhesive electrodes (Superior Silver Electrodes, Uni-patch, MN, USA) were cut to 2.5 cm x 1.0 cm for each muscle. The distal electrode for TA and MG was placed just proximal to the tendon - muscle interface with the other two electrodes placed proximal on the muscle belly, each separated by 4 cm. The distal electrode for vastus lateralis was placed approximately 13 cm proximal to the patella. Electrodes for biceps femoris muscle were placed on the midline of the posterior leg and aligned with the vastus lateralis electrodes as shown in Fig. 4.1.

The electrodes were secured to the skin covering the muscles using medical grade tape (Hypafix, Smith & Nephew Pty Ltd, Victoria, Australia) and subsequently wrapped with several layers of athletic tape (Co-flex, Andover Healthcare, MA, USA) to ensure that the electrodes stayed in the same position during the entire 24 hour EMG recording.

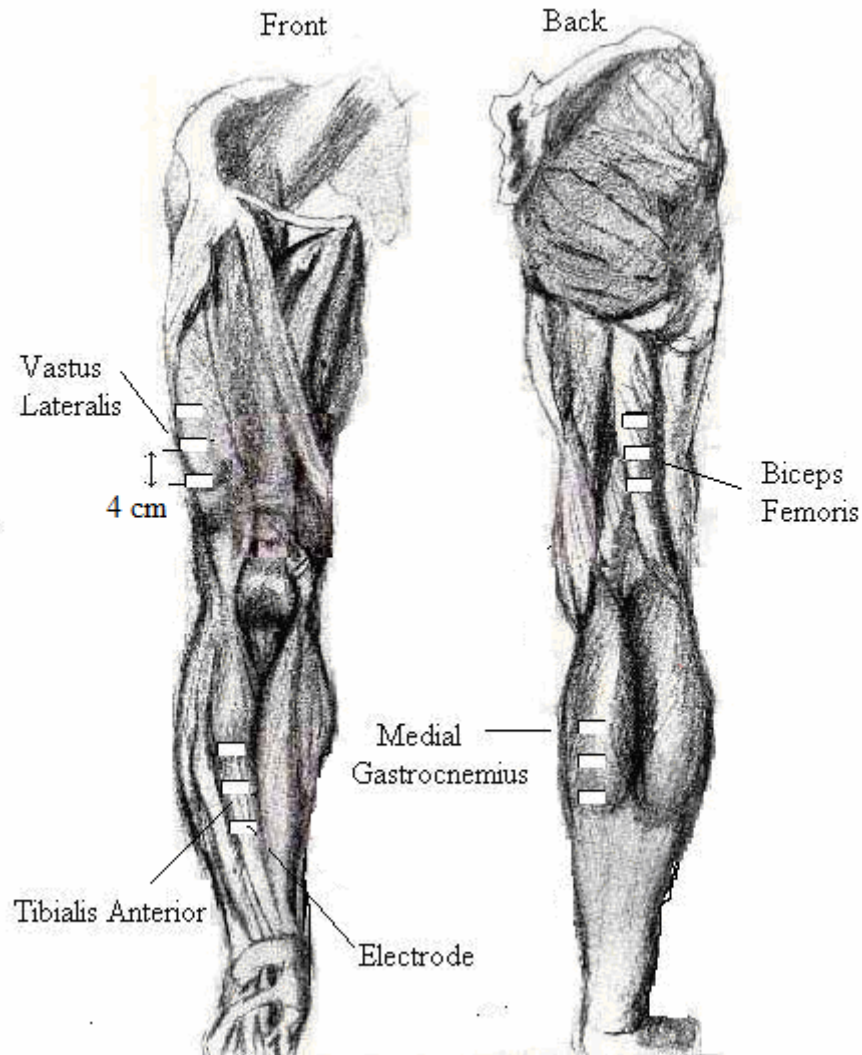


Fig. 4.1. Electrode configuration employed for the four leg muscles (modified from paintings of Amanda Jo Ellingson, www.amandajoellingson.com).

4.1.2 Logger setup

The electrodes from each muscle were connected to preamplifiers (Motion Control, Salt Lake City, Utah, gain approximately 400). The outputs from the four preamplifiers for each leg were connected to a custom built preprocessing box which was responsible for filtering (30-500 Hz) and amplifying the input signal to fit the input range

of the data logging device. The outputs from each preprocessing box ($n=2$, one for each leg) were connected to a custom built portable, battery operated, data logging device capable of simultaneously recording 8 channels of EMG signals (Fig. 4.2).

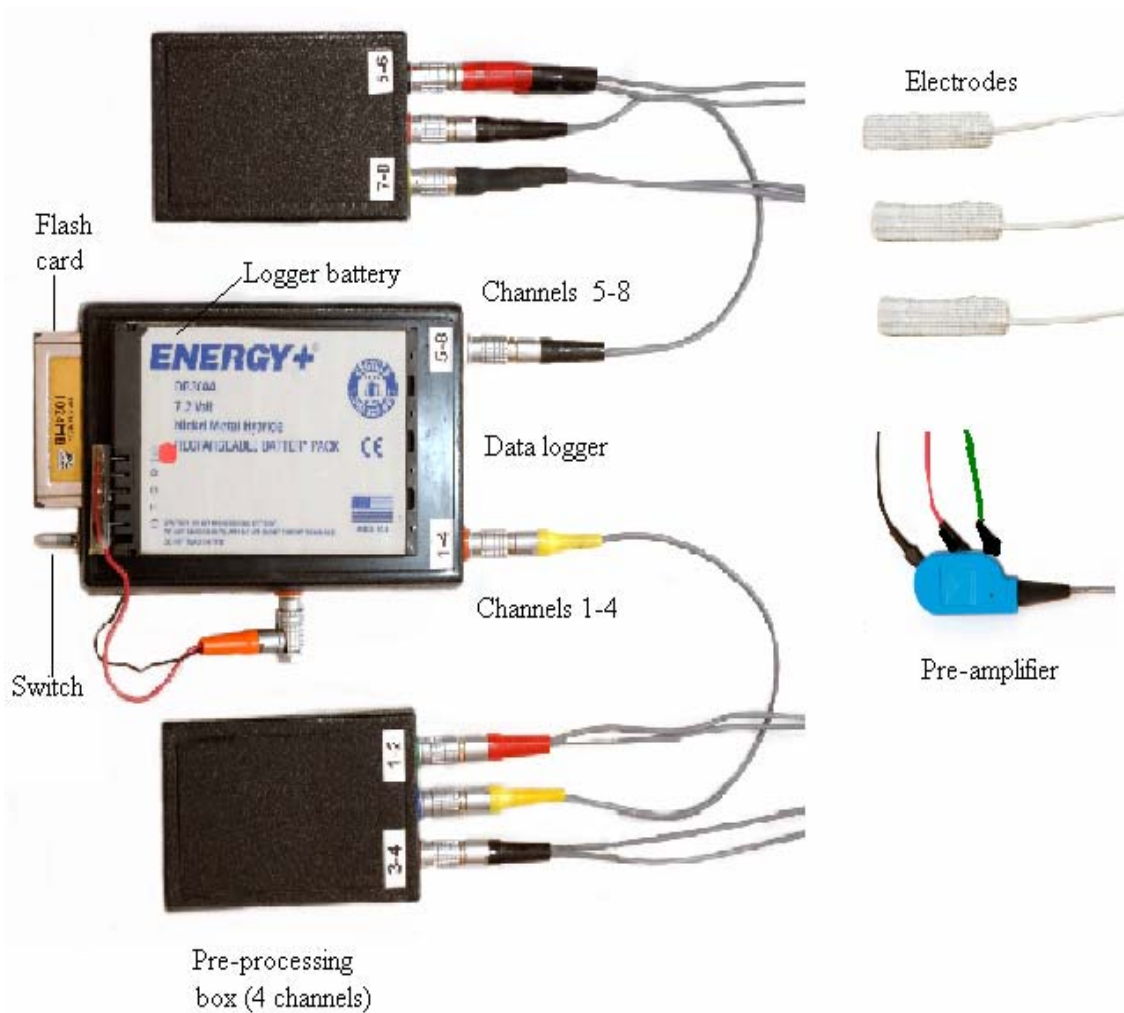


Fig. 4.2. Equipment for recording 24 hour EMG signals from 8 muscles.

The data logging device consists of a Tattletale 8 Logger (Onset Computer Corporation, Bourne, MA) driven by custom software written using Metrowerks Code Warrior (a C based software development tool). The data logger uses a 12-bit analog to digital converter that allows the inputs signals to range from 0 to 4.096 V. The sampling

rate was 1000 Hz per channel. The data were written to a 1 GB compact flash card in compressed format.

4.1.3 Calibration

Each channel was calibrated prior to and after the 24 hour data collection by recording a 1 mV sine wave at 100 Hz from a signal generator to the data logger for 30 seconds. These readings were used to relate the input voltage supplied and the voltage recorded by the logger. The calibration procedure was repeated after the 24 hour recording to account for changes over time due to draining of batteries. In addition calibration also accounts for the gain (amplification) from the amplifiers in both the logger and SC/Zoom system. For example an input signal of 1 mV to the logger records a signal close to 400 mV. Similarly a 1 mV signal input to Zoom records a signal ranging from 0.9 - 1 mV. The difference in the actual and the recorded values is attributed to the gain of the amplification circuitry involved in both the logger and SC/Zoom systems. The calibration factors are obtained by taking the ratio between the two values, correcting for the units of measurement and by averaging the pre and post values. After calibration a 1 mV recorded signal is equivalent for both the logger and SC/Zoom.

4.1.4 Stimulation protocol

Prior to and after the 24 hour recording, data were collected in the laboratory. Maximal compound muscle action potentials (M waves) were recorded from vastus lateralis (VL), tibialis anterior (TA) and medial gastrocnemius (MG) muscles in response to supramaximal stimulation of the femoral, common peroneal and tibial nerves, respectively (Thomas 1997). The area under the maximal evoked M-waves before and

after the 24-hour recording were similar indicating stability of the recording electrodes over the entire recording which means the changes in activity in each muscle are recorded faithfully. These EMG data were recorded on-line (1000 Hz) using a SC/Zoom system (Physiology section, Umeå University, Sweden).

4.1.5 24 hour EMG recording

After the stimulation protocol, a 20 minute trial recording was made to test the function of the data logging equipment. During this short recording the subjects were asked to trigger leg spasms including clonus, move in their wheel chair, lift their legs and lean back. Meanwhile the subject was advised to maintain his/her normal routines during the 24 hour recording to ensure a representative view of daily activities. Instructions were also given about how to reduce noise in the recordings from external sources such as electronic devices or cell phones. The 24 hour recording was initiated by switching on the toggle switch on the logger and by giving commands to start recording from the computer via a RS-232 port. The data logger was stored in a hip pack. A flashing LED on the data logger indicated that the recording was in process. The subject returned after 24 hours to participate in the post recording stimulation protocol.

4.1.6 EMG Processing

Prior to analysis of the EMG data, six processing steps were implemented. 1) The recorded data were copied to a computer and each channel extracted to 24 1-hour files of data using a custom extraction program developed in MATLAB. 2) The data for each channel were set to the 24 hour clock where midnight to 1 am was designated as hour 1; 3) 60 Hz notch FIR filtering followed by 30 Hz FIR high pass filtering to eliminate noise

were implemented on all data. Both filters have order 472 and are linear phase to avoid distortions. The filter coefficients were calculated from the built-in Kaiser functions in Ddsp. Coefficients for the 60 Hz notch filter were obtained with the following parameters (sampling frequency = 1000 Hz, lower cutoff frequency = 55 Hz, upper cutoff frequency = 65 Hz, stop band attenuation at 40 dB). The 30 Hz high pass filter was obtained at a sampling frequency of 1000 Hz and a lower cutoff frequency of 25 Hz with a stop band attenuation of 40 dB. Programs were developed in MATLAB using these filter coefficients to perform filtering operations on an offline basis. 4) EMG data were calibrated to obtain a signal that is equivalent for both the logger and SC/Zoom. 5) artefacted to remove further noise from the data; 6) spasms were manually categorized as (i) tonic for sustained EMG; (ii) units for train of motor unit potentials; (iii) clonus for rhythmic, repeating contractions at a frequency of 3-8 Hz; (iv) myoclonus for contractions repeating at a frequency of 0.5-3Hz; and (v) mixed for combinations of some of these spasm types. All of these processing routines had been developed in MATLAB and were executed on an off-line basis. Only EMG data labeled as clonus or a mixed spasm were considered in this study.

4.2 Algorithm to detect the onset and offset of each burst of EMG during clonus

Three cycles of clonus, with the onset and offset of the EMG marked manually by lines, are shown in Fig. 4.3. The process of using software to automatically determine the start and end of EMG during user defined spasms that include clonus are described in the subsequent sections of this chapter. The basis of this detection method is derived from the technique of “intensity analysis” proposed by Vincent Von Tscherner (2000). The results of this method are used to calculate the duration of the EMG during each clonus cycle (On duration), clonus frequency, and the magnitude of the EMG in each clonus cycle. All of these parameters are used to characterize clonus.

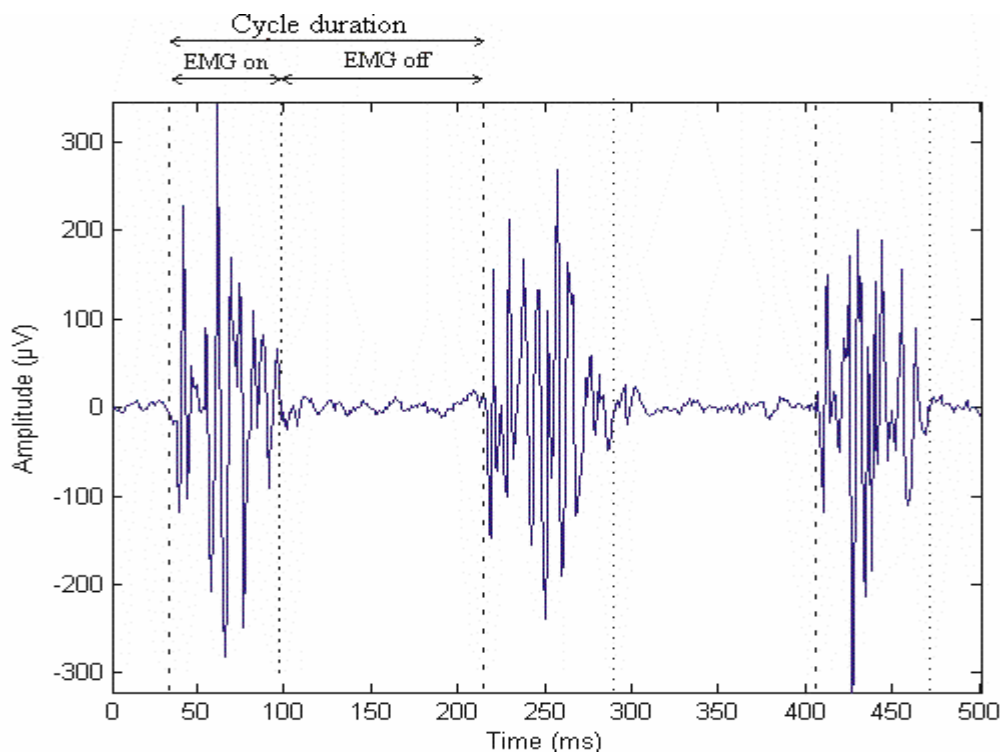


Fig. 4.3. The start (...) and end (...) of each EMG burst marked manually during 3 cycles of clonus recorded from the right medial gastrocnemius muscle during hour 14 (1-2 pm; Subject F, injury at C4).

Five steps are involved in the algorithm used to detect the start and the end of the EMG during each cycle of clonus (Fig. 4.4).

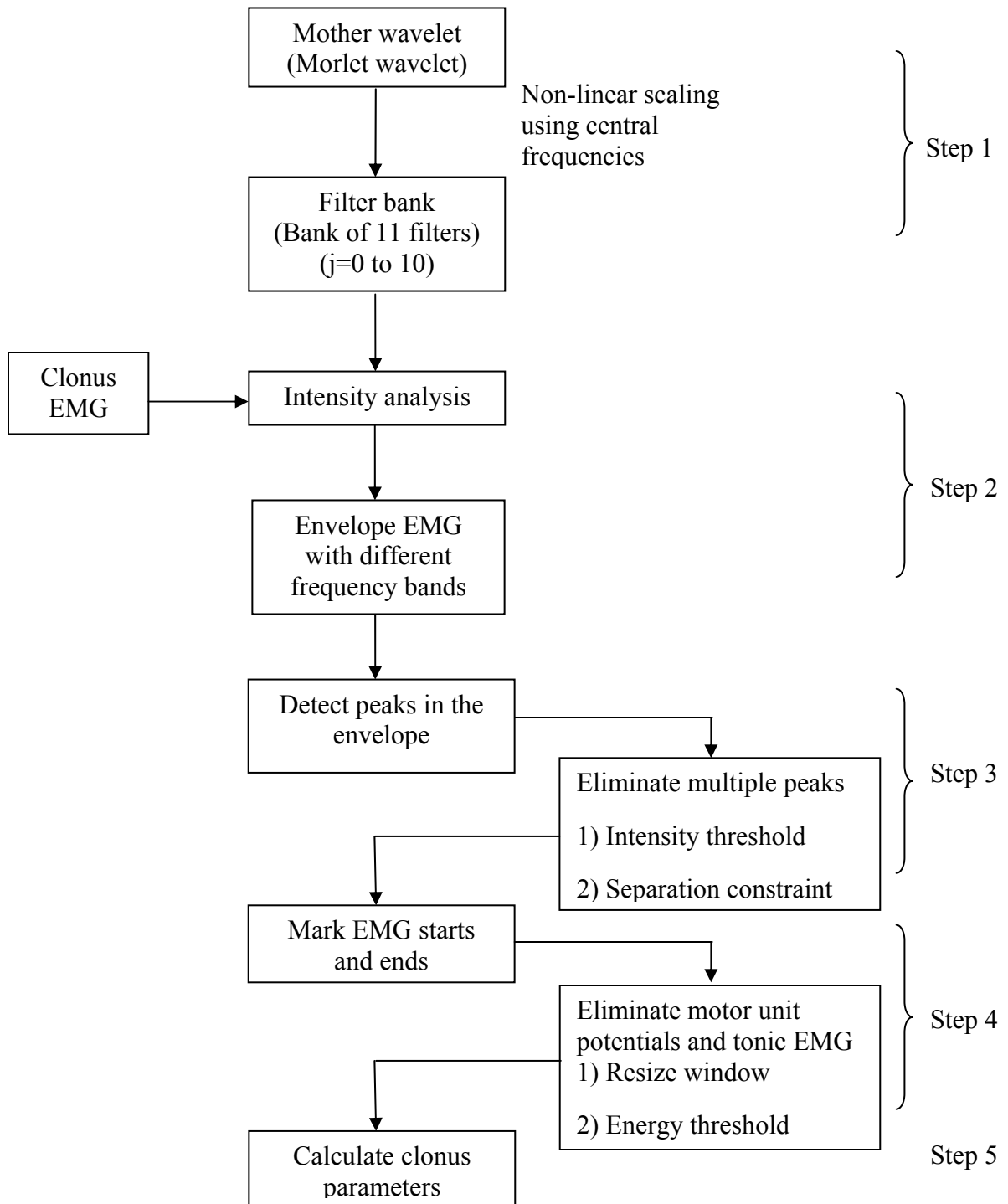


Fig. 4.4. Flow chart of the detection algorithm.

4.2.1 Step 1: Creation of a bank of filters using the Morlet wavelet

In this analysis, the Morlet wavelet is used to create filters for analyzing the intensity of the EMG. A filter is created by non-linear scaling of the mother wavelet (Morlet wavelet) using a central frequency (Table 4.2). The time and frequency domain representation of the scaled wavelets (filters) are given by the following equations:

$$\varphi(t) = \sqrt{\frac{\alpha \cdot cf}{2\pi}} \cdot e^{i2\pi cf t - \alpha cf \frac{t^2}{2}}$$

$$F\varphi(f, cf, scale) = \left(\frac{f}{cf}\right)^{cf \cdot scale} \cdot e^{i\left(\frac{f}{cf} + 1\right) \cdot cf \cdot scale}$$

Where: α is defined as $4\pi/scale$,

Scale is a scaling factor that defines the frequency range covered by each wavelet (scale=0.3).

cf is the central frequency given by:

$$cf(j) = \frac{1}{scale} \cdot (j + q)^r$$

Where: j ($j=0, 1 \dots 10$) is the index of the wavelet that defines the entire frequency range examined.

Parameters q and r ($q=1.45, r=1.959$) are used to optimize the spacing between the filters with narrow frequency ranges covered at lower frequencies.

Table 4.2. Central frequencies

Wavelet index (j)	Central frequency (Hz)
0	6.90
1	19.29
2	37.71
3	62.09
4	92.36
5	128.47
6	170.39
7	218.07
8	271.49
9	330.62
10	395.44

A set of 11 filters was created by scaling the mother wavelet to form a bank of filters. Each filter has a normalized amplitude of 1.0 at its central frequency. For example, the filter $j=3$ has an amplitude of 1 at its central frequency of 62.09 Hz (\downarrow symbol in Fig. 4.5). At the same frequency the sum of the amplitudes of the other filters is approximately 0.33, resulting in a total amplitude of 1.33. Another criterion for optimization is that adjacent wavelets overlap enough to cover the frequency range of EMG signals without gaps (20-400 Hz). For the summed filters in Fig. 4.5 the pass band is from 0-450 Hz. The time resolutions of the filters range from 12.0 ms to 76.5 ms (Von Tscharner 2000). The time resolution of filters should be close to the physiological response time of the muscle (10-100 ms) for the analysis of EMG. The range for physiological response time is based on observations made on reactions observed during vertical jumps and unintended activation of muscles (Von Tscharner 2000).

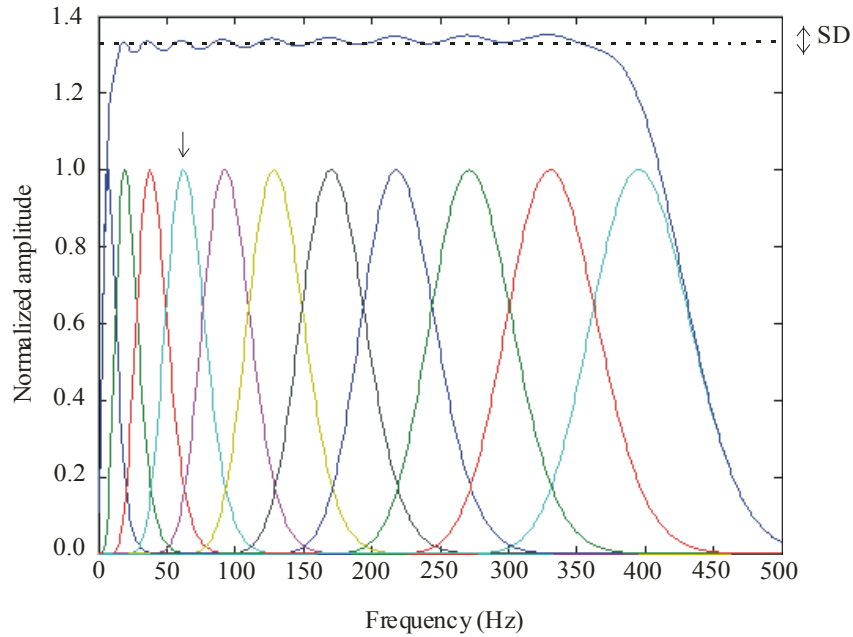


Fig. 4.5. Filter bank of 11 wavelets ($j=0$ to 10) in the frequency domain. The sum of all of the wavelets covering the entire range of EMG frequencies (top trace). The mean value (---) and SD (\updownarrow) of the summed filter.

4.2.2 Step 2: Intensity analysis to envelope EMG

The EMG data are passed through a series of 11 different band pass filters to produce the intensity of the signal as a function of both frequency and time. This process is mathematically represented as a convolution in the time domain or by a simple multiplication in the frequency domain given by the equation:

$$FW_j = F\Psi_j . FS$$

Where: FW_j is the wavelet transformed signal,

$F\Psi_j$ is the Fourier domain representation of the filter,

FS is the Fourier domain representation of the EMG signal.

As a result of this filtering operation, the EMG is decomposed into different frequency bands. The summation of these filtered signals is a close approximation of the original EMG signal within the accuracy given by the standard deviation ($SD = 0.009$) of the sum of all of the filters (Fig. 4.5).

The squared filtered signals produce waveforms that envelope the EMG (Fig. 4.6). The signal is squared to approximate the power of the EMG signal at a particular time 't'. In this case, the voltage $V(t)$ is recorded from the muscle that is assumed to have a constant resistance, R . Then the instantaneous power $P(t)$ is given by:

$$P(t) = \frac{V(t)^2}{R}$$

The entire process of producing these intensity envelopes for all of the 11 frequency bands is carried out in MATLAB. The output is presented graphically to the user for the entire duration of the clonus (Fig. 4.6).

The filters generate multiple oscillations in the envelopes because they are sensitive to short term changes in the EMG. To eliminate some of these oscillations, the envelopes can be summed together into different groups. Here, the 11 envelopes were combined into 3 different groups. The lower frequency bands were obtained by adding the envelopes from filters $j = 1, 2, 3$, intermediate frequency bands by adding the envelopes from filters $j = 4, 5, 6$, and higher frequency bands by adding the envelopes

from filters $j = 7, 8, 9, 10$. The intensity obtained by using filter $j=0$ has no significant value because the input signal was filtered prior to this analysis (30 Hz high pass).

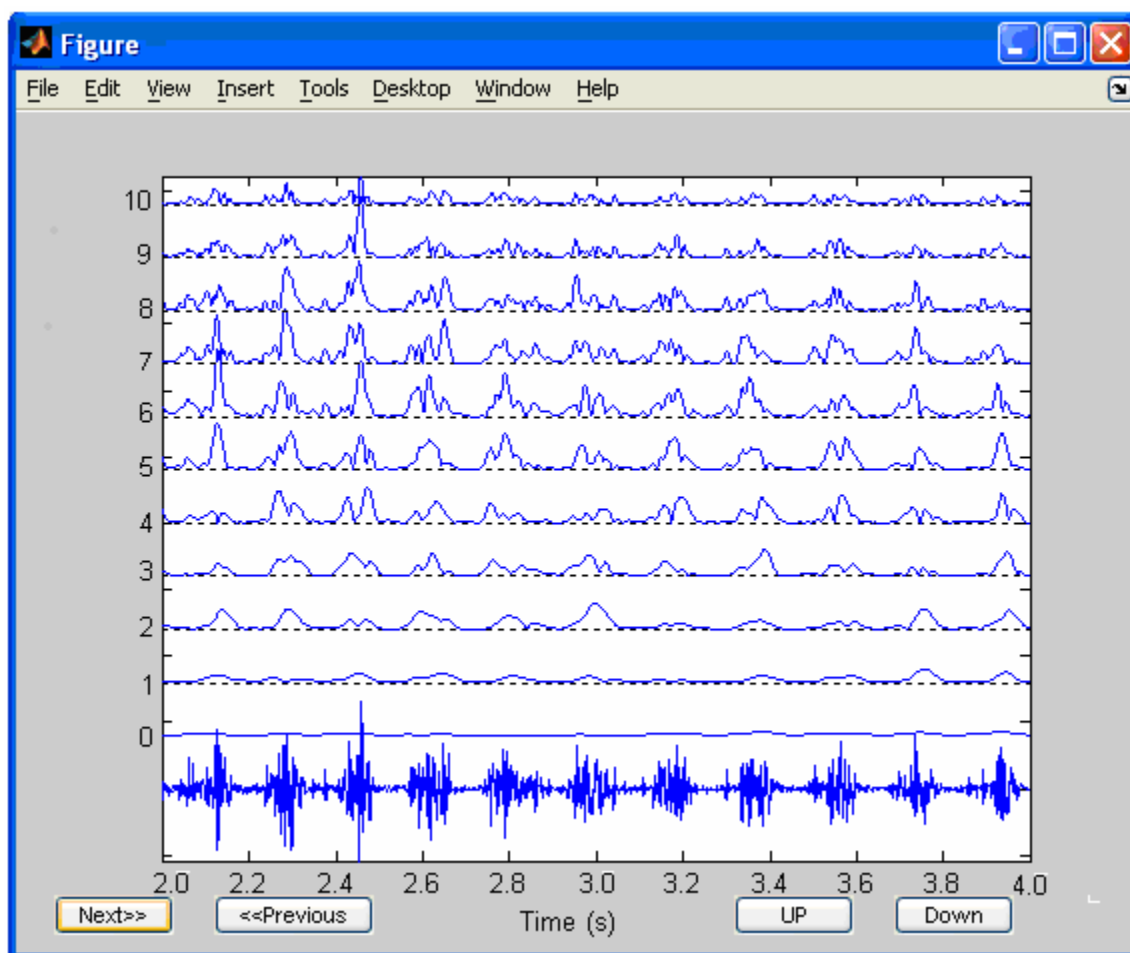


Fig. 4.6. User interface to view the 11 intensity envelopes and the EMG signal (bottom trace). The user can increase or decrease the signal magnitude and can scroll forward or back through the data. The EMG was recorded from the left medial gastrocnemius muscle during hour 21 (8-9 pm; Subject F, injury at C4).

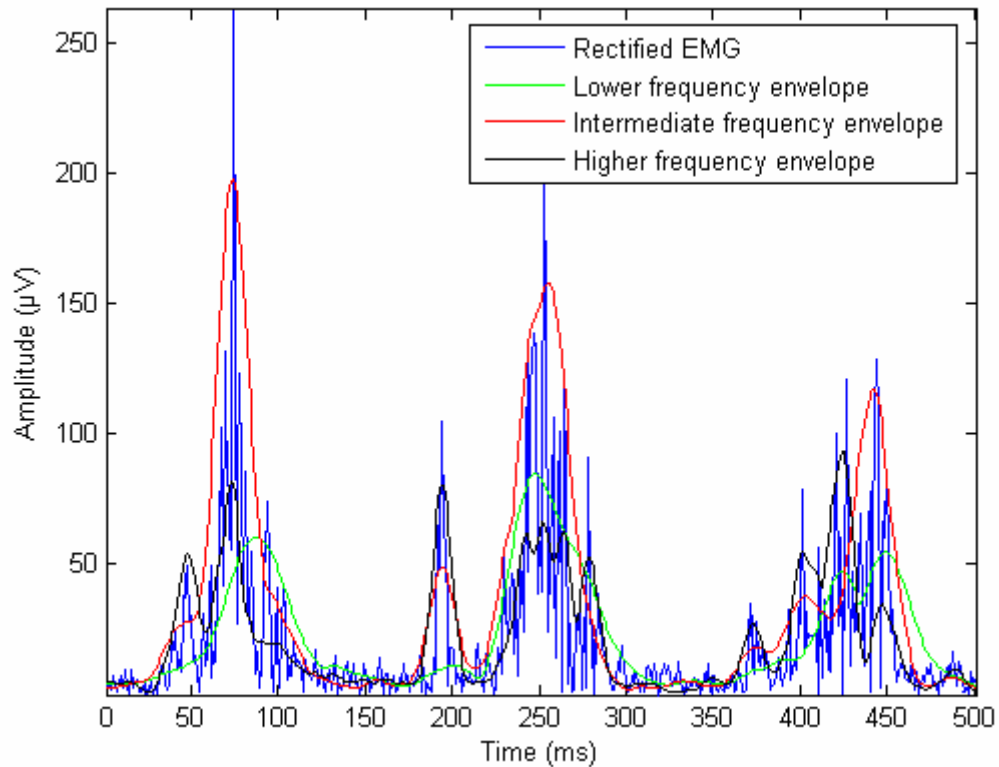


Fig. 4.7. Linear envelopes to the rectified EMG (blue) for lower frequency (green), intermediate frequency (red), and higher frequency bands (black). The EMG was recorded from the left medial gastrocnemius muscle during hour 21 (8-9 pm; Subject F, injury at C4).

Combining envelopes helps to increase the efficiency of the algorithm as the combined envelopes closely follow the EMG. An example of the lower, intermediate and higher frequency envelopes is shown in Fig. 4.7 in relation to the rectified EMG. Notice that all three envelopes follow the EMG signal. However, the lower frequency envelope reacts slowly to the changes in the EMG so there is a delay in it following the EMG. In contrast, the higher frequency envelope is highly reactive to the changes in the signals, producing multiple peaks in the envelope. The intermediate frequency envelope, which is moderately sensitive to the input signal, offers a compromise between the two other

envelopes in terms of sensitivity to changes in the EMG and the production of multiple peaks. In addition, the intermediate frequency envelope largely represents the frequencies ranging from 80-190 Hz (i.e., the lower cut-off frequency (-3 dB) of filter (j=4) and the upper cut-off frequency (-3 dB) of filter (j=6)). Hence the envelope for intermediate frequencies is preferred for subsequent analysis. However, as discussed in subsequent sections of the chapter (Step 4) the lower frequency envelope is used to adjust for motor units firing between the bursts. The higher frequency envelope is eliminated from the analysis.

4.2.3 Step 3: EMG burst detection

Each burst of EMG is reflected as one or more peaks in the envelope. An algorithm was developed to determine the time at which peaks occurred in the envelope. This was accomplished by calculating the slope of the waveform at each instant by determining the first derivative of the signal and observing the changes in the value of the slope. The slope increases in the direction of the peak, becomes zero at the peak and decreases after the peak.

Without any constraints, the algorithm identifies the peaks of interest and smaller peaks that reflect motor unit activity, baseline noise, or changes in EMG. To reduce the detection of multiple peaks for each burst of EMG, two constraints were imposed on the algorithm:

- 1) An intensity threshold was needed to differentiate between the EMG and the baseline. In order to determine this threshold the data were viewed using Dadisp software (DSP Development Corporation, Newton, MA) by overlaying the rectified EMG and the

intensity envelope. Different threshold values ranging from 15-30 μV^2 were used to separate the baseline from EMG. For 95% of the data observed, the threshold was 25 μV^2 . Hence this value was used as a constraint to eliminate peaks from the baseline in all records.

2) A time constraint between adjacent peaks was also used to avoid detection of multiple peaks due to changes in EMG or motor unit activity. Different examples of clonus were studied. The number of bursts of EMG in the entire spasm involving clonus was counted manually and compared to the peaks identified by the algorithm. The value of the time constraint between peaks was progressively changed from 40 ms to 120 ms in steps of 10 ms and the peaks detected by the algorithm recounted. Based on these observations a minimum separation of 90 ms between the peaks was found to be optimal for most recordings in this study. In an example of clonus from subject F shown in Fig. 4.8, 63 EMG bursts were observed manually. A total of 78 peaks were identified by the algorithm using a separation constant value 40 ms. Successively increasing the separation constant between peaks in steps of 10 ms to a value of 90 ms, resulted in the algorithm identifying the same 63 bursts which were manually identified.

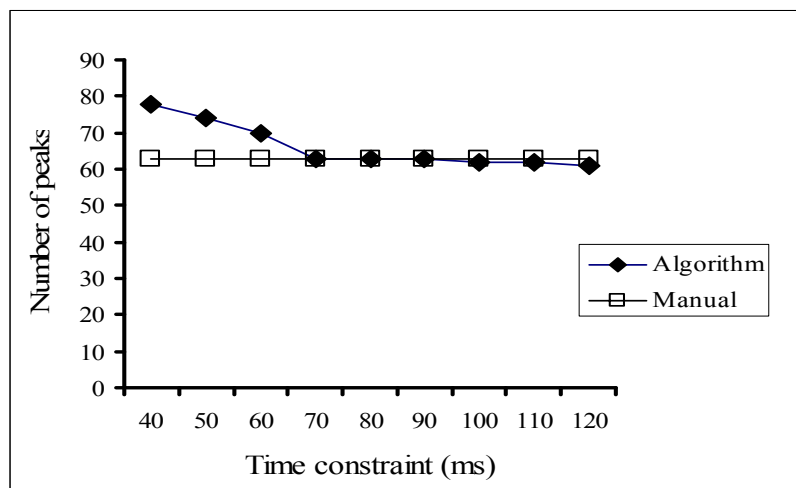


Fig. 4.8. Number of peaks identified by the algorithm by successively changing the time constraint until the result matches the number of peaks identified manually. The EMG was recorded from the left medial gastrocnemius muscle during hour 21 (8-9 pm; Subject F, injury at C4).

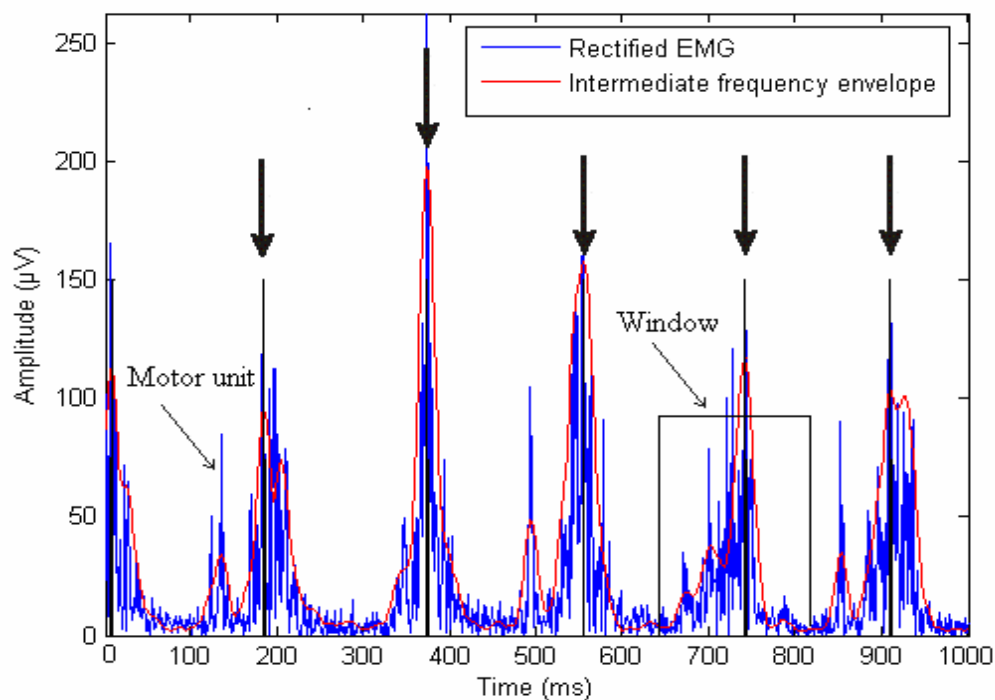


Fig. 4.9. Peak detection (down arrows) in rectified EMG (blue) with the intermediate frequency envelope (red). The EMG was recorded from the left medial gastrocnemius muscle during hour 21 (8-9 pm; Subject F, injury at C4).

4.2.4 Step 4: Marking onset and offset of EMG bursts

A window is placed around each peak detected by the algorithm, from the midpoint of the previous peak to the midpoint of the next peak (Fig. 4.9). Thus, the entire record is covered with consecutive windows. The total energy of the EMG signal in each window is then computed using the equation:

$$\text{Energy} = \sum_{t=W_s}^{W_e} |X(t)|^2$$

Where: $X(t)$ is the EMG signal,

W_s is the beginning of the window,

W_e is the ending of the window.

The point at which the energy in the window reaches a value of 5% of the total energy is marked as the start of the burst of EMG. Like-wise, the point at which the energy in the window reaches 95% of the total energy represents the end of the burst of EMG. Energy values less than 5% of the total energy usually correspond to the baseline noise. When the burst amplitudes were low, this 5-95% criterion was automatically changed to 10-90%. Using this condition improves the accuracy of detecting bursts with low amplitudes.

Eliminating motor unit potentials firing in between EMG bursts Use of the window method to mark the start and end of the EMG is appropriate for most bursts of EMG. However in certain recordings, motor units that fire in between the bursts of EMG

are included (Fig. 4.10) because they respond early to the muscle stretch and spindle activity (Wallace et al. 2005). These motor units are not part of the burst but they contribute to the energy in the window. To eliminate this motor unit activity from the burst of EMG, the detection window was resized to 50 data points (50 ms) on either side of the EMG peak. This resizing of the window was based on data from subjects A and F, recordings in which motor unit activity typically fired 60-80 ms before the actual EMG burst. It is known from the literature that the typical duration of the EMG burst is in the range of 40 -70 ms (Dimitrijevic et al. 1980) indicating that resizing the window had little negative effect in determining the start and the end of the burst. The start and end of the EMG bursts are then marked with respect to the resized window by calculating energy contained within the resized window as described earlier. The difference between the two windows and the actual start and end times for one burst of EMG are shown in Fig. 4.10.

In other recordings there was a lot of motor unit activity in between the EMG bursts. For these special cases the user was provided with an option to indicate to the algorithm that there was a high incidence of motor unit activity between the bursts of EMG. When this option was selected the algorithm employed the lower frequency envelope instead of the intermediate frequency envelope to identify the EMG bursts. This approach improved the detection of the EMG burst because the motor unit potentials were less pronounced in the lower frequency bands.

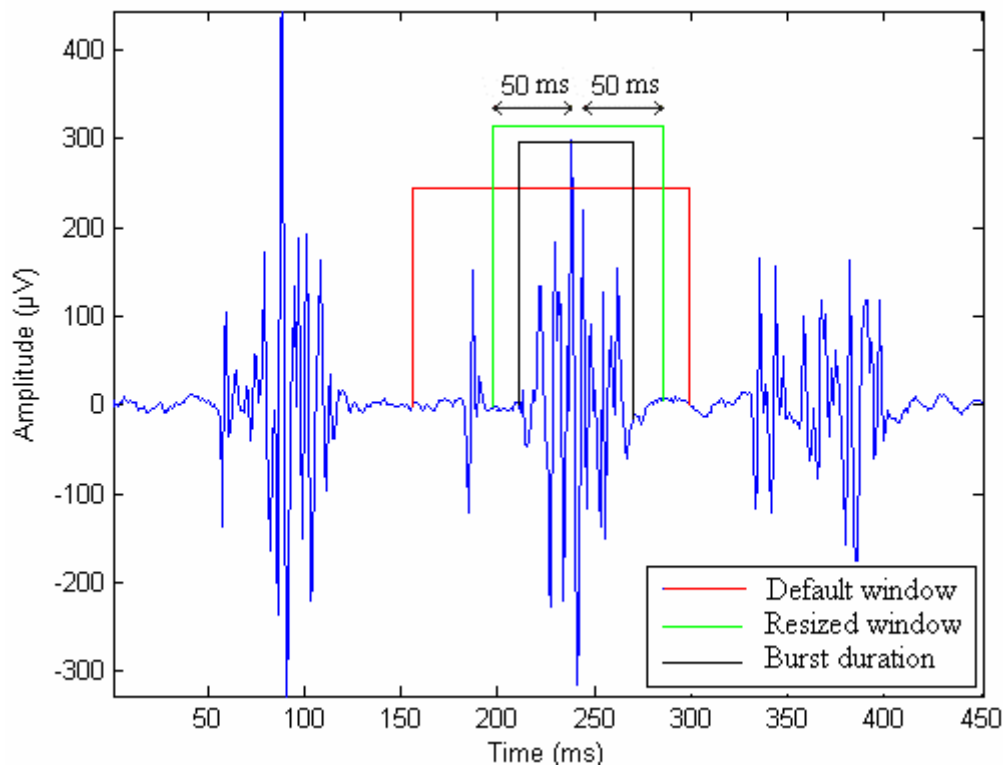


Fig. 4.10. Three bursts of EMG with a default window (red box), resized window (green box) and the start and end of the EMG (black box) after applying the resized window. The shorter window excludes the motor unit potential from the burst of EMG. The EMG was recorded from the left medial gastrocnemius muscle during hour 15 (3-4 pm; Subject F, injury at C4).

Eliminating motor unit potentials and tonic EMG Certain spasms begin with either a series of motor unit potentials, a tonic burst of EMG or some combination of these signals rather than clonus. In such cases only a part of the spasm provided to the algorithm involved clonus. The period of clonus that was to be analyzed needed to be defined. To eliminate the motor unit activity prior to the start of clonus, the total energy of each burst was calculated. The energy associated with motor unit potentials is much smaller than that of a burst of EMG during clonus. A threshold value for energy was used for eliminating these motor unit potentials. In all 7 experiments, energy typically ranged

from 5-15 mV^2 for motor unit potentials. A threshold value of 7.5 mV^2 was found to eliminate these motor unit potentials in the majority of cases.

Tonic EMG typically exceeds 150 ms. However with the resized window size described in the section “Eliminating motor unit potentials firing in between EMG bursts”, the detected burst duration cannot exceed 100 ms. In such cases the algorithm breaks tonic EMG into 2 or 3 EMG bursts which are closely separated. To identify tonic activity, the bursts separated by a duration less than or equal to 30 ms are merged (added together) to capture the tonic EMG. If these merged bursts have a duration greater than the threshold of 160 ms, they are treated as tonic EMG and discarded. The values for these constraints were obtained by manually observing the data from the subjects E and F and progressively changing the constraints to obtain the desired output from the algorithm.

For example one clonus from subject F had 53 bursts assessed by manual count. There were 7 motor unit potentials, and a tonic burst of EMG before the clonus began and 1 motor unit potential at the end of clonus (Fig. 4.11). Without the constraints, the algorithm identified a total of 63 bursts and with the constraints the algorithm identified 53 bursts because the motor unit potentials and tonic burst were eliminated.

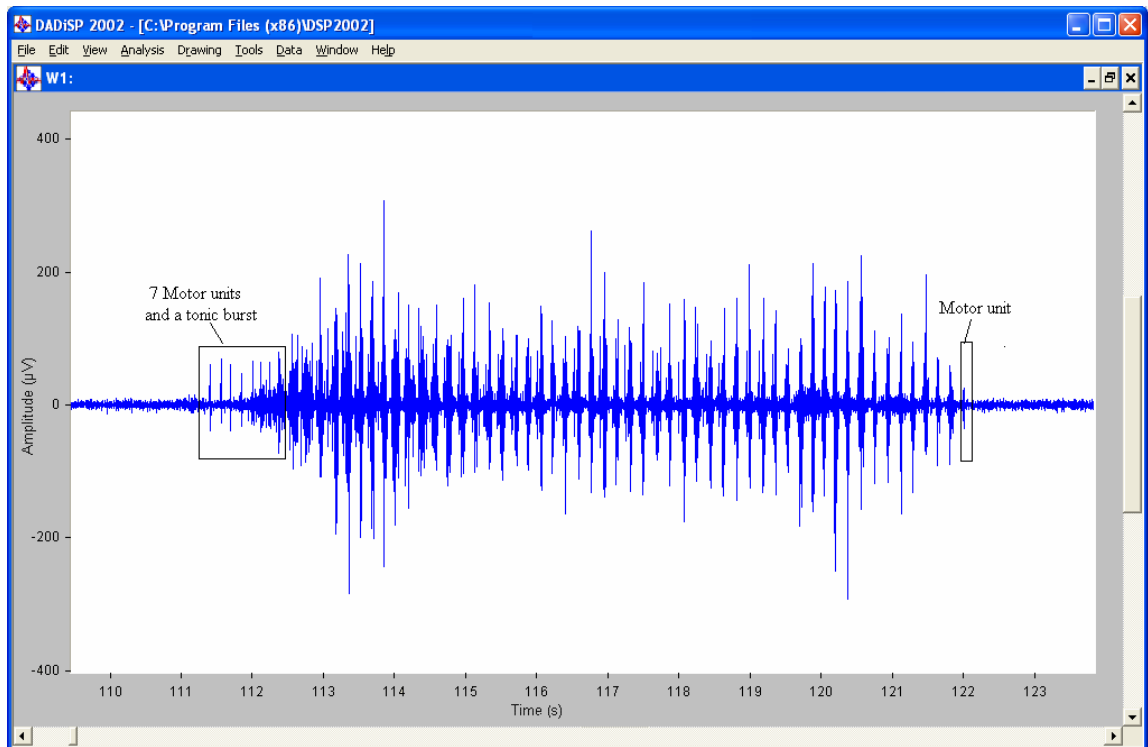


Fig. 4.11. Motor unit potentials ($n=7$) and a tonic burst of EMG at the beginning and a motor unit potential at the end of the clonus. The EMG was recorded from the left medial gastrocnemius muscle during hour 21 (8-9 pm; Subject F, injury at C4).

4.2.5 Step 5: Calculation of clonus parameters.

The start and end times for each burst of EMG during clonus were used to calculate three parameters:

- 1) EMG duration (On duration), the time from the start to the end of the EMG burst (Fig. 4.3).

2) Clonus frequency given by the equation:

$$\text{Clonus frequency} = (1/\text{cycle duration}) * f_s$$

Where: f_s is the sampling frequency of the EMG signal.

3) EMG intensity, the root mean square value (RMS) for each burst of EMG.

The output of the entire algorithm is a text file that contains the channel number, the hour of the recording, the EMG start time and EMG end time for each burst of EMG during each spasm involving clonus.

4.3 Manual measurements

In this study the performance of the algorithm was analyzed quantitatively by comparing the output produced by the algorithm (i.e., the start and the end of each burst of EMG during clonus, on duration, clonus frequency and the RMS value of each burst of EMG during clonus) to that obtained manually by two people. Each human operator was required to mark the start and end of each burst of EMG during clonus independently. In this study the start and end of each burst of EMG from 5 spasms involving clonus were manually viewed and marked per subject (n=7) except for subject D who had only 1 clonus in the entire 24 hr recording. The same spasms were measured independently by two different operators. These manually determined starts and ends were used to calculate on duration, clonus frequency and RMS value of the EMG burst and compared to the output produced by the algorithm developed in this study.

A MATLAB based user interface was developed by linking MATLAB programs and Dadisp software (DSP Development Corporation) so that the user could select the desired file, view the data, and make the manual measurements (Fig. 4.12). The interface provides user friendly features such as push buttons, text boxes, check boxes and radio buttons to enter the desired values and to display to the data in a Dadisp window either as rectified or unrectified EMG depending upon the option selected by the user. An example of the EMG display is shown in Fig. 4.13.

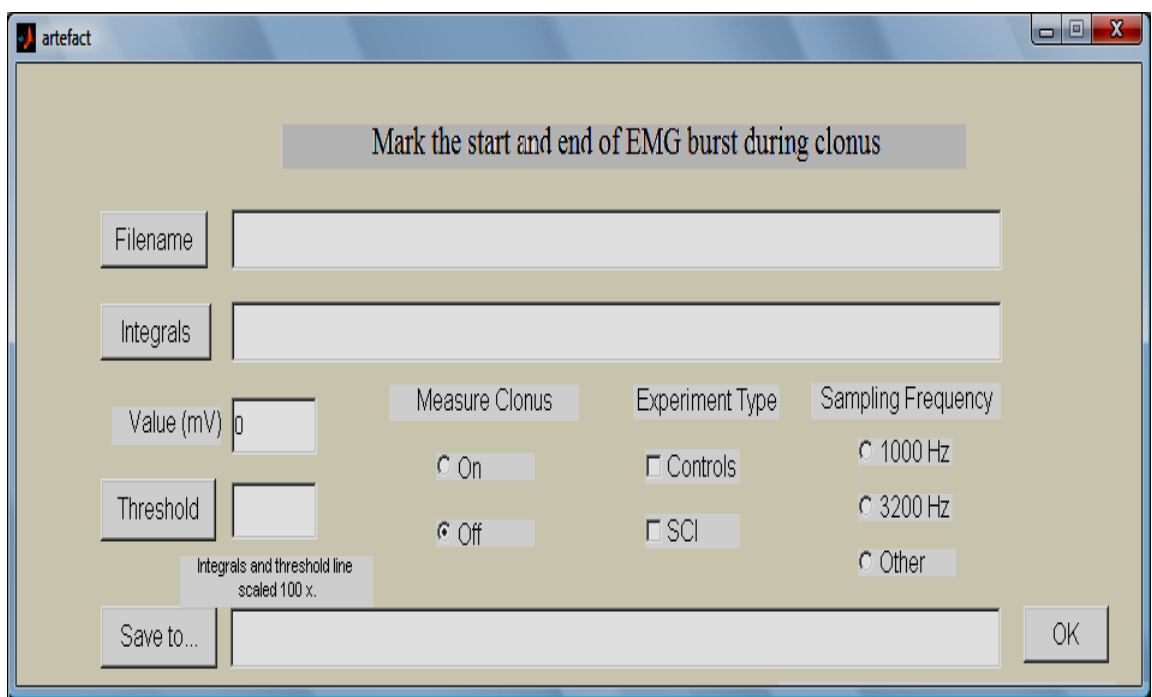


Fig. 4.12. User interface to view the EMG data and manually mark the start and the end of each EMG burst during clonus.

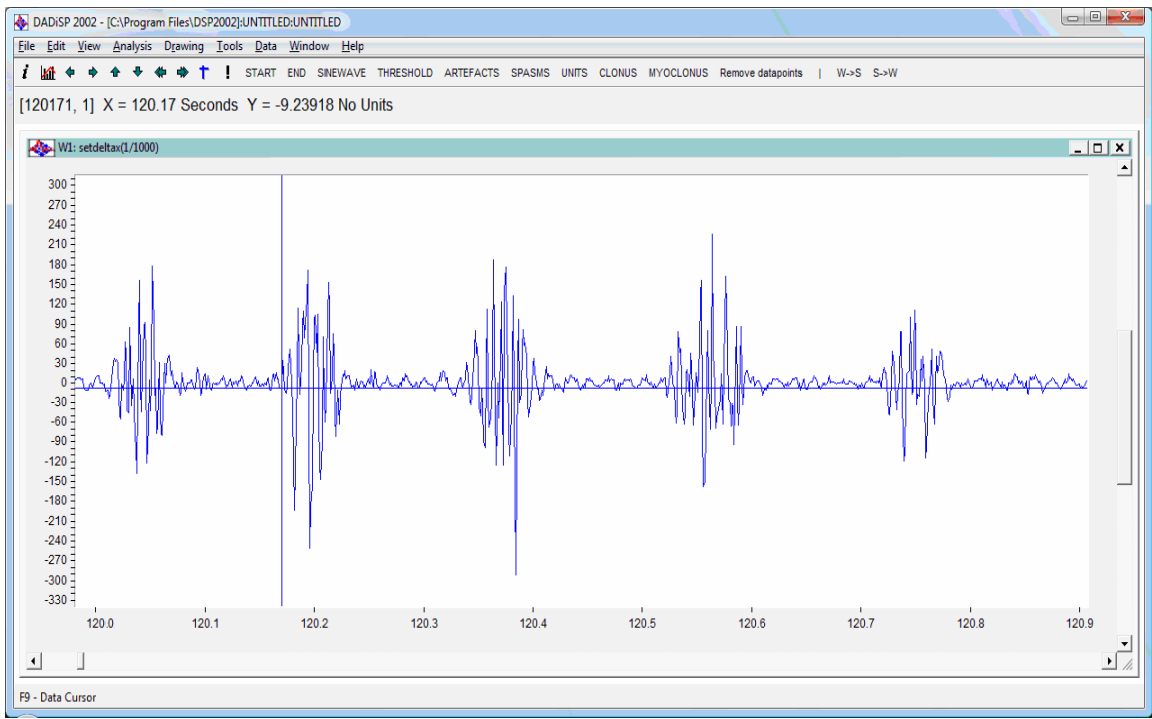


Fig. 4.13. Dadisp window produced by the interface for the user to view and mark the start and end of EMG bursts manually. The cross-wire points to the start of a burst of

EMG and the mark is registered to the output file. The EMG was recorded from the left medial gastrocnemius muscle during hour 21 (8-9 pm; Subject F, injury at C4).

In the Dadisp window, the user is provided with many tools (default features of Dadisp software) which are quite similar to that of the Windows operating system. In addition the user can zoom in, zoom out, magnify and scroll across one hour of data (Fig. 4.13).

Manual marking of the start and end of each burst of EMG. To register the start and end of each burst, the user needs to click and register the start and end of the EMG with the cross hairs, then the clonus option in the top menu (see Fig. 4.13). Thus, to mark each EMG burst it takes five operations. Repeating this process to register all EMG bursts during clonus is time consuming and requires a great deal of concentration. A custom made MATLAB program was used to read the cross-wire location when the start and end buttons in the tool bar were clicked and to these points to a text file.

Output file The text file output produced by the interface includes channel number (1-8), hour number (1-24), as well as the start and the end of each burst of EMG in the clonus.

4.4 Visual comparison of measurements

The starts and ends of bursts of EMG marked by two different operators and the algorithm can be viewed simultaneously to evaluate the decisions. A MATLAB user interface was developed to display the EMG and the outputs in Dadisp (Fig. 4.14).

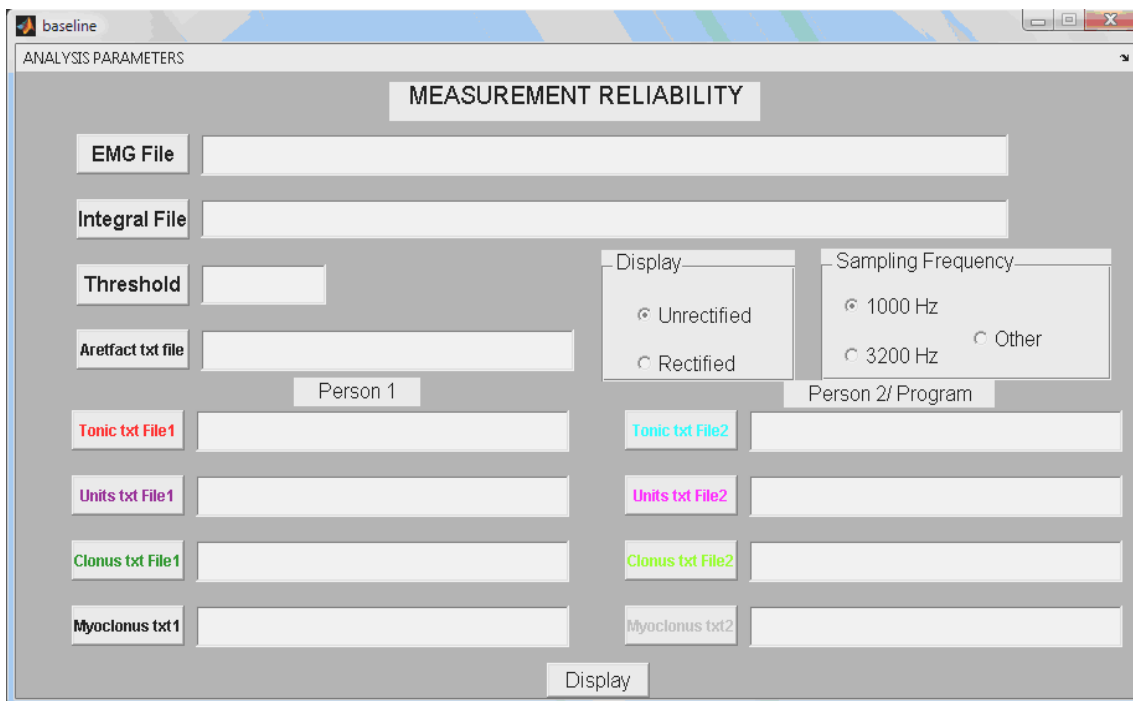


Fig. 4.14. User interface to select and visually compare the measurements produced by different operators or a person and the algorithm.

This program converts the readings in the text files into a pulse signal equal in length to that of the EMG file (1 hour). The time between each start and end reading is set to 1 while the remaining values are set to zero. The EMG file and the pulse signal are overlaid and displayed in a Dadisp window using different colors (Fig. 4.15). In the Dadisp window, the measurements made by Person 1 are displayed at 50X magnification and the data from Person 2 or the Program are displayed at 100X magnification. An

example of this display is shown in Fig. 4.15 for the markings made by Person 1 and Person 2 on the same data. Notice the two operators differ in marking the start time and end time for the first and second bursts largely due to the inclusion or exclusion of a motor unit potential.

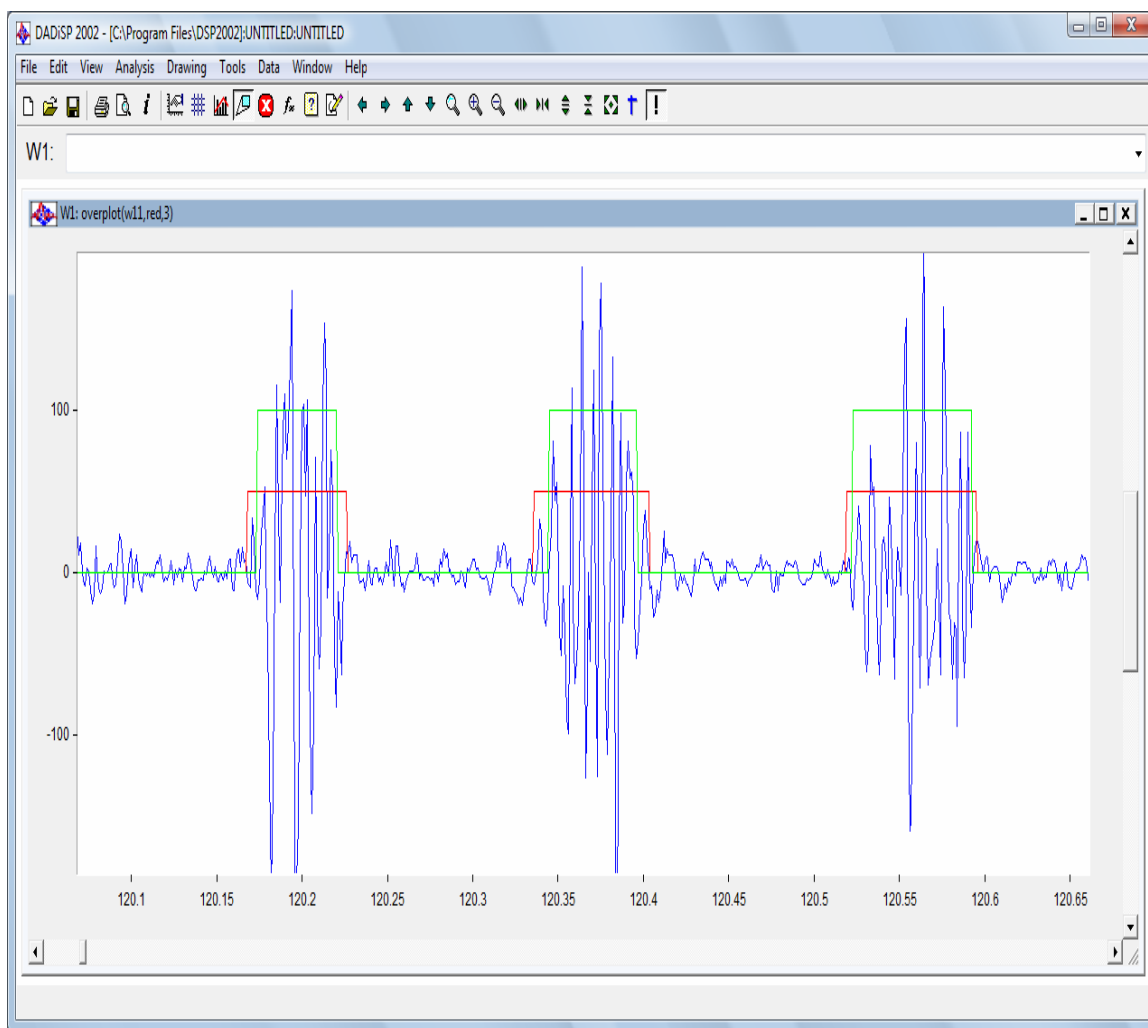


Fig. 4.15. The display output produced by the user interface to compare the performance of operator(s) and/or an operator and the program. Red markings indicate the decisions made by Person 1 and the green markings were made by Person 2. The EMG was recorded from the left medial gastrocnemius muscle during hour 21 (8-9 pm; Subject F, injury at C4).

4.5 Comparison of outputs from the algorithm and human operators

To compare the measurements made by the two individual operators and the algorithm, a template was developed in Microsoft Excel. Person 1 was set as the standard and comparisons were made between Person 1 and Person 2 (P1 Vs P2), and Person 1 and the Program (P2 Vs Pr). Data from Person 2 and the Program were also compared but not reported in this study, because Person 2 developed the algorithm. Hence the comparisons were treated as biased. This excel template also served as the source of data for all statistical analyses carried out to verify the performance of the algorithm.

4.5.1 Template structure and organization

The template was set to accommodate 5 spasms from each subject and a maximum of 200 EMG bursts per spasm. Formulae were used to calculate On duration, clonus frequency, the number of EMG bursts for Person 1, Person 2 and the Program, relative start and end times, the difference or agreement between these parameters for data from Person 1 and Person 2, and Person 1 and the Program. The data were also shown graphically.

4.5.2 Data transfer to the excel template

Transfer of data to the template was achieved by using programs developed in MATLAB. To make this data transfer process more user friendly, a user interface was developed so that the user could select the files, transfer data to the template and save the template in a location specified by the user (Fig. 4.16). This process reduced both the time and potential errors that would occur with manual data entry. The user just needed to

navigate to find the data files and click the OK button to perform the data transfer operation.

The screenshot shows a software window titled 'clonus' with three distinct sections for data processing:

- Transfer rates and program output for comparison:** This section contains five text input fields labeled 'EMG Filename', 'Person1txt file', 'Person2txt file', 'Programtxt file', and 'Save to'. An 'OK' button is located to the right of the 'Save to' field.
- Single clonus analysis:** This section includes an 'EMG Filename' field, 'Start point' and 'End point' fields, a 'Threshold' field with the value '25', and an 'MU threshold' field with the value '7500'. It also features two radio button groups: 'Motor unit' (with 'Yes' and 'No' options, 'No' is selected) and 'View multi channels' (with 'Yes' and 'No' options, 'No' is selected). A 'Save to' field and an 'OK' button are at the bottom.
- Analyze all channels and hours:** This section has four text input fields: 'First filename', 'Lastfilename', 'Text file', and 'Save to'. It includes a 'Motor unit' radio button group (with 'Yes' and 'No' options, 'No' is selected), 'Threshold' (25) and 'MU threshold' (7500) fields, a 'Next batch' button, and three checkboxes: 'Analyze', 'Compare across channels', and 'Export to excel'. An 'OK' button is at the bottom right.

Fig. 4.16. User interface to transfer the output text files produced by the operators and the algorithm for each spasm into the excel template for comparison (top), to perform analysis of a single clonus (middle) and to analyze clonus from 24 hour records (bottom).

This program is independent of filename but dependent on the file path provided by the user. The spasms measured in this study are distributed across 24 hours and 8 channels (muscles). To handle this wide variation the program is developed to access all the files produced for a particular subject and writes data sequentially into the Excel

template. This data transfer program also calculates and writes the RMS value of each EMG burst using the start and the end values from the original data file.

4.6 Automatic clonus analysis by the algorithm

4.6.1 Single clonus analysis

The start and end times for the EMG bursts in one clonus can be obtained by using the single clonus analysis section of the user interface (Fig. 4.16; middle). The user has to select the path of the EMG data file and enter the beginning and the end time of the clonus. Default values for the intensity threshold ($25 \mu\text{V}^2$) and motor unit threshold (7.5mV^2) are displayed but can be changed depending on the nature of the data. The user can also choose whether to have the algorithm adjust for motor units between bursts.

4.6.2 Analysis of clonus in 24 hr recordings

Analysis of clonus in 24 hour recordings from multiple muscles can be carried out using the 'Analyze all channels and hours' section of the user interface (Fig. 4.16; bottom). This interface allows the user to analyze data from a single hour, some hours, or all 24 hours of a single muscle. Data from multiple muscles can be analyzed in batches.

The entire analysis can be run using this batch processing feature of the program, where the user has to create the batches by selecting the first and last file to be analyzed and the text file with timing information of clonus for the selected files. This batch processing section can be used to perform two different operations. 1) to analyze data from multiple muscles; 2) to export analyzed data into the excel template. The program takes 5-15 minutes to analyze 24 hours of data from one muscle depending on the

complexity and amount of data and 2-5 minutes to write the data from a single muscle into the excel template.

Output files The output text files produced for the 24 hours of data need to be checked and corrected for discrepancies by adjusting start and end times with the aid of Dadisp software. In this study 24 hour analysis was performed on the data from one single muscle (right medial gastrocnemius) of subject F (injury at C4). The analysis output text files were transferred into another master template to summarize the results. The template was set to accommodate data from all 24 hours, a maximum of 17 spasms with clonus in any one hour of data, and a maximum of 400 EMG bursts per spasm. Formulae to calculate On duration, clonus frequency and the magnitude of EMG bursts were included as explained for the template used to compare inter-rater outputs.

4.7 Statistics

Statistical analyses were performed using SPSS-17.0 software (SPSS Inc, Chicago, IL) and Sigmastat software (Systat Software, San Jose, CA). Two comparisons were made on the results: 1) between Person 1 and Person 2; 2) between Person 1 and the Program, to evaluate whether the algorithm was as good as a human operator in terms of its performance in analyzing clonus.

Kruskal-Wallis one way ANOVA on ranks was used to demonstrate the agreement in identifying the number of EMG bursts identified during each spasm involving clonus, to test whether the algorithm was faster than the human operators at analysis, and to determine whether the number of EMG bursts, on duration, clonus frequency and intensity of contractions during clonus were different during awake and

sleep times of the 24 hour recording. Common times for on durations (the duration of EMG burst that was common to the measurements of the operators or the operator and the program), clonus frequency, and the RMS values of EMG bursts during clonus were subjected to reliability analysis. Intra-class correlations (ICC) were calculated to verify the inter-rater reliability of the measurements (model-3 i.e., the two-way mixed effect module). ICC coefficients can range from 0 (no agreement) to 1 (perfect agreement). In general, a value greater than 0.80 is regarded as satisfactory (Shrout and Fleiss 1979, Nunnally and Bernstein 1994). To verify whether the differences between the operators and the operator and the algorithm were statistically significant, Chi-square tests were performed. Statistical significance was set at $p < 0.05$. Data are presented as means (\pm SE) unless stated otherwise. Standard error was used to express variance about the population mean. The count (n) is also included, so the SD can also be derived.

Chapter 5: Results

5.1 Performance evaluation

In this study, a total of 31 spasms involving clonus were analyzed by the program and manually by two different human operators. The algorithm developed in this study was evaluated for its performance in 6 ways by comparing the results of two people (Person 1, P1; Person 2; P2) to the data obtained from Person 1 and the Program (Pr). Comparisons made were: 1) the number of common bursts of EMG identified as clonus; 2) differences in the start and end times of bursts of EMG; 3) agreement on On duration, 4) agreement for clonus frequency; 5) agreement on the RMS value of the EMG during the bursts of EMG; 6) the time taken to measure the start and the end times of EMG bursts during clonus.

5.1.1 Number of common bursts of EMG

The number of common EMG bursts measured for each clonus were compared by the percentage agreement between the program and Person 1 & the two operators. For example Person 1 and Person 2 both measured 54 bursts of EMG in one spasm from subject G, so were in 100% agreement. The algorithm analyzed 56 bursts of EMG, 53 of which were the same as Person 1 so the algorithm agreed 98% of the time with Person 1. On a subject-by-subject basis, agreement varied between 94-100% for the measurements made by Person 1 and Person 2, and varied between 92-100% for Person 1 versus the algorithm (Fig. 5.1).

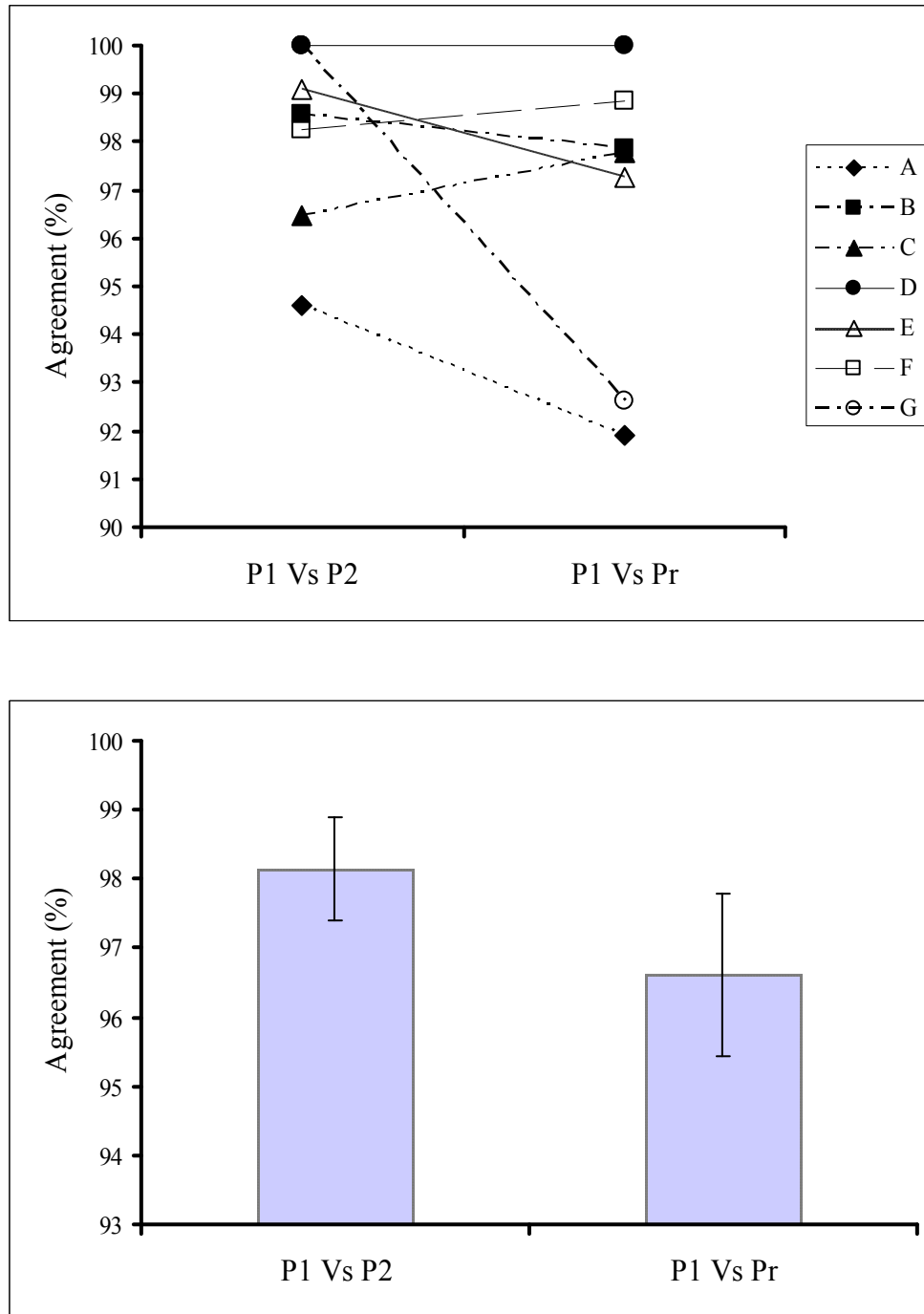


Fig. 5.1. Percentage agreement on number of common bursts analyzed by Person 1 and Person 2 (P1 Vs P2) and Person 1 and the algorithm (P1 Vs Pr) by subject (top). Mean (\pm SE) agreement on common EMG bursts ($n=7$ subjects; bottom).

For the group data, average agreement was 98% (SE 1) between the two operators, and 96% (SE 1) between Person 1 and the algorithm. The differences in agreement were not significant ($p=0.946$). Thus the algorithm was as effective as two humans in identifying the bursts of EMG during clonus.

5.1.2 Start and end time differences

The start time and end time of each burst of EMG during clonus were measured by both operators and the algorithm. The time difference between the start and end times of EMG bursts were compared to assess Person 1 to Person 2 and Person 1 to Program performance. A typical example of start time and end time comparisons are shown in Fig. 5.2. The closer the values are to the zero line, the closer the agreement between the measurements. A positive value means that Person 1 marked a time after Person 2 or the Program, whereas a negative value indicates that Person 1 measured a time before Person 2 or the Program. The start and the end time comparisons shown in Fig. 5.2 indicate that, on average, both Person 2 and the Program vary by ± 10 ms when compared to Person 1 in marking starts and ends of EMG bursts, the typical duration for a motor unit potential (Thomas et al. 2006).

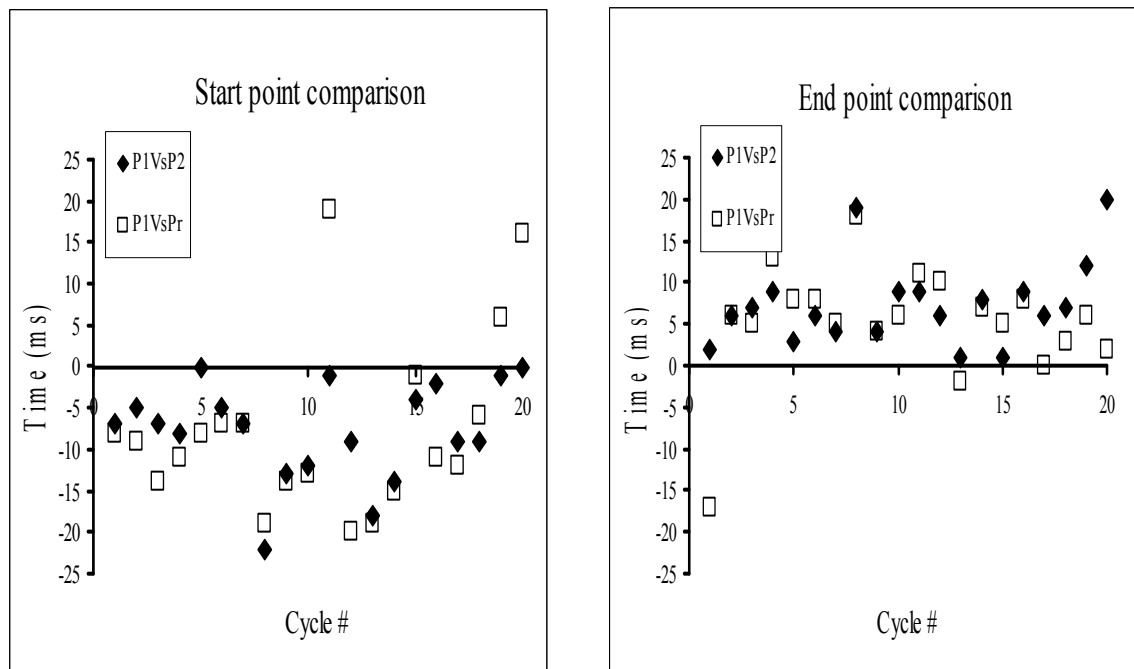


Fig. 5.2. Start time (left) and end time (right) differences between P1 and P2 and P1 and Pr for one clonus recorded from the left medial gastrocnemius muscle during hour 8 (7-8 am; Subject C, injury at C6).

Histograms were produced to show the distribution of time differences for the start time and the end time measurements made by the operators and the program. Histograms are obtained on a spasm-by-spasm basis. The percentage of data in each bin was calculated, averaged to get the mean distribution of the data for each subject and plotted with respect to the mid points of the bins (i.e., the data sets falling in the 0-10 ms bin are represented at 5 ms, as shown in Fig. 5.3). Histograms obtained for the start time difference from 5 different spasms of subject C are shown for Person 1 and Person 2 in Fig. 5.3. The mean distribution for subject C indicates that for 81 % (SE 2) of the measurements, Person 2 marked a start time that was up to 10 ms later than Person 1, a difference in time that is the approximate duration of one motor unit potential.

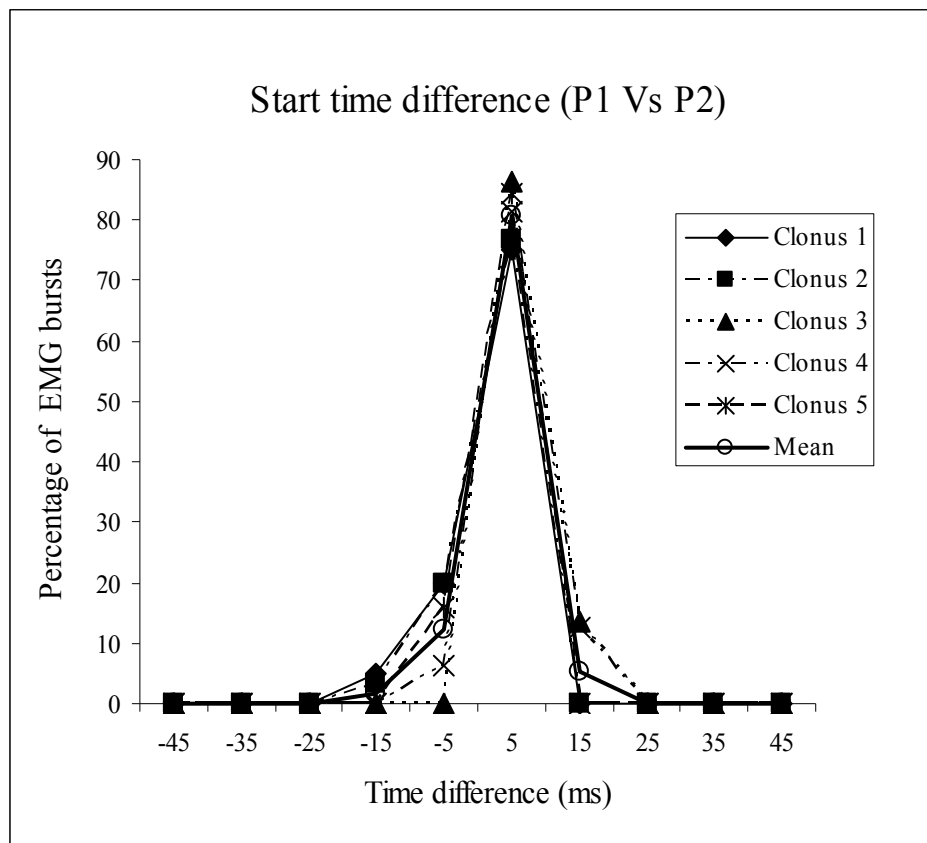


Fig. 5.3. Histograms for the start time difference between Person 1 (P1) and Person 2 (P2) for data from subject C (n=5 spasms and mean data).

Group data for start time (Fig. 5.4) and end time (Fig. 5.5) indicates that differences in identifying the start and end times of the EMG bursts differed in most cases by less than ± 10 ms for the human operators and the program. The start times for Person 1 and Person 2 differed by ± 10 ms for 71% (SE 3) of cases (n = 854). For end times it was 57% (SE 5) of cases. The corresponding data for Person 1 and the Program were 57% (SE 6) and 51% (SE 3).

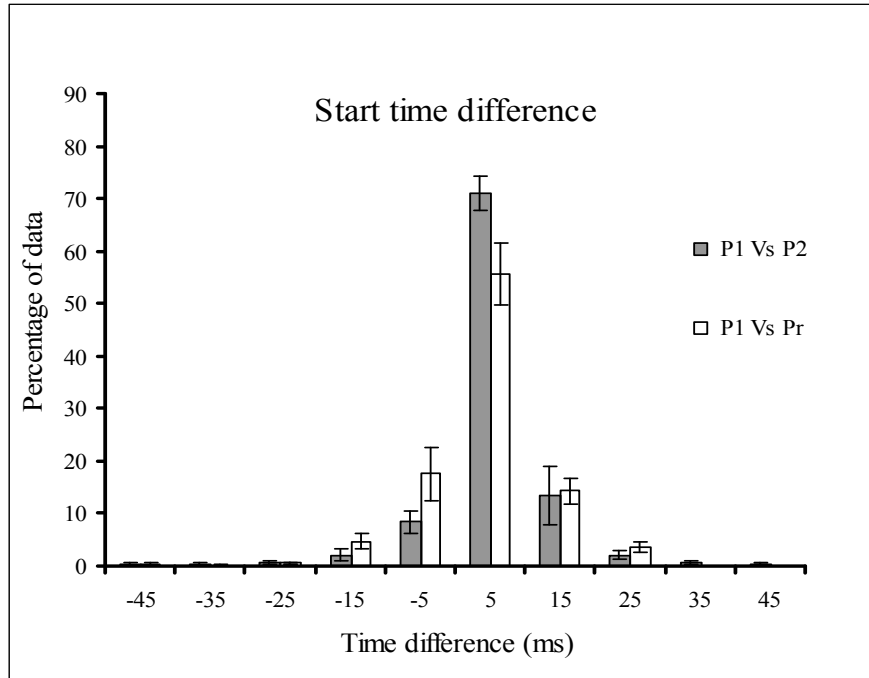


Fig. 5.4. Histograms of mean (\pm SE) start time differences between human operators and Person 1 and the program.

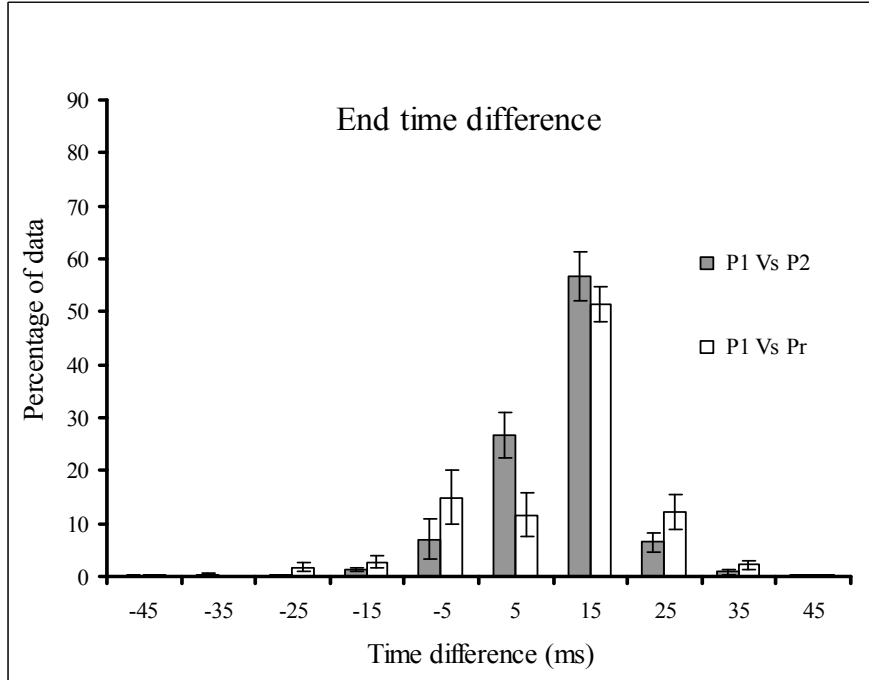


Fig. 5.5. Histograms of average (\pm SE) end time differences between human operators and Person 1 and the program.

5.1.3 Discrepancies in start and end times

In 72 cases out of 854 (8.4%) the difference between the start times or the end times were greater than 25 ms. Such cases were considered discrepancies. The 42 discrepant start times and 30 end times were viewed with the aid of Dadisp software to identify the potential cause for each discrepancy.

Seven reasons were identified for the discrepant start and end times. The reasons included:

1. Motor unit potentials: When a motor unit potential is close to the EMG burst it can be included or excluded in the EMG burst either by a person or the program. The program considers a motor unit potential as part of the EMG burst when the potential falls within the resized window (± 50 ms on either side of the detected peak).
2. Filtering: After effects of the filters (60Hz notch, 30 Hz high pass) employed in the preliminary EMG processing sometimes resulted in a slow wave before and after the EMG, resulting in early start and late end times by the program.
3. Inter-burst EMG: In some clonus there was EMG between the primary bursts of EMG which sometimes was included in marking start or end times by the program.
4. Big motor unit potential: In some clonus, a big motor unit potential could alone contribute a large amount of energy to the window region resulting in an early start and/or end times.

5. Misjudgements: Both people and the program misinterpret the start and end of the EMG burst.
6. EMG bursts of low amplitude: In some clonus the amplitude of the EMG bursts was low. In these cases, the program generally generated longer end times as more data points were needed to reach 90% of the energy of the window.
7. Poor interference pattern: Some EMG bursts had a poor interference pattern. That is, the EMG was more distinct motor unit potentials rather than fused potentials resulting in start or end time discrepancies by the program.

Most of the discrepancies in start or end times were caused by motor unit potentials followed by filtering effects and inter-burst EMG activity (Fig. 5.6). Motor unit potential discrepancies were relatively high in subjects A and F because of the prevalence of motor unit activity in these recordings.

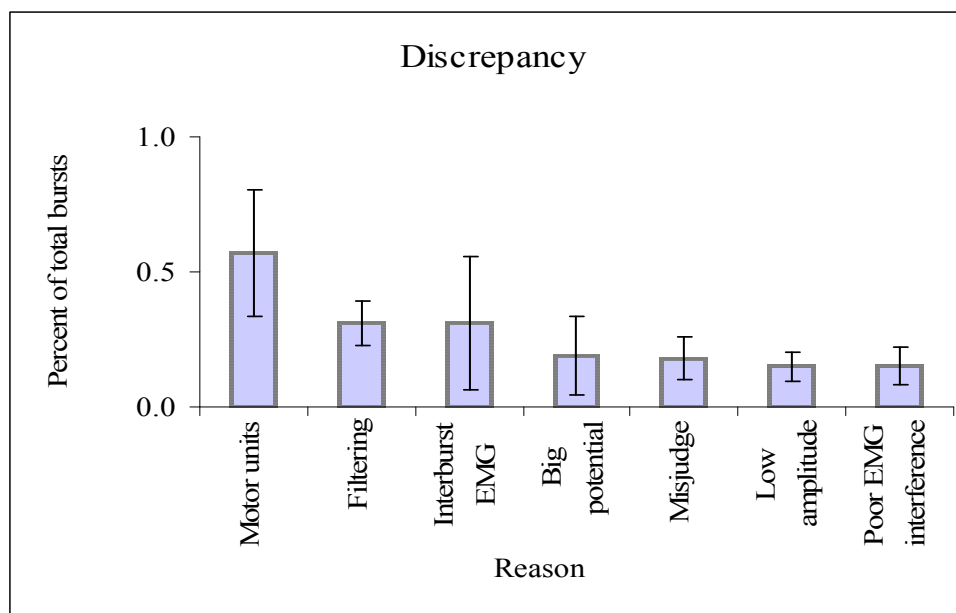


Fig. 5.6. Mean (\pm SE) percent of total bursts with discrepancies in start and end times for group data represented on a per spasm basis for each of the 7 subjects.

5.1.4 On durations

The time between the start and the end of the EMG represents the time of the EMG burst or on duration. The on duration for each EMG burst was calculated from the measurements of the human operators and the program. The on durations from one clonus (Fig. 5.7) show Person 1 consistently measured longer durations than either Person 2 or the Program. On average, on durations were 56 ms (± 8), 41 ms (± 8) and 43 ms (± 12) for Person 1, Person 2 and the Program, respectively. In terms of evaluating algorithm performance, the percent agreement for on duration or common time was measured. Agreement for on duration in this example was 73% (SE 3) between Person 1 and Person 2, compared to 72% (SE 3) between Person 1 and the Program (Fig. 5.8).

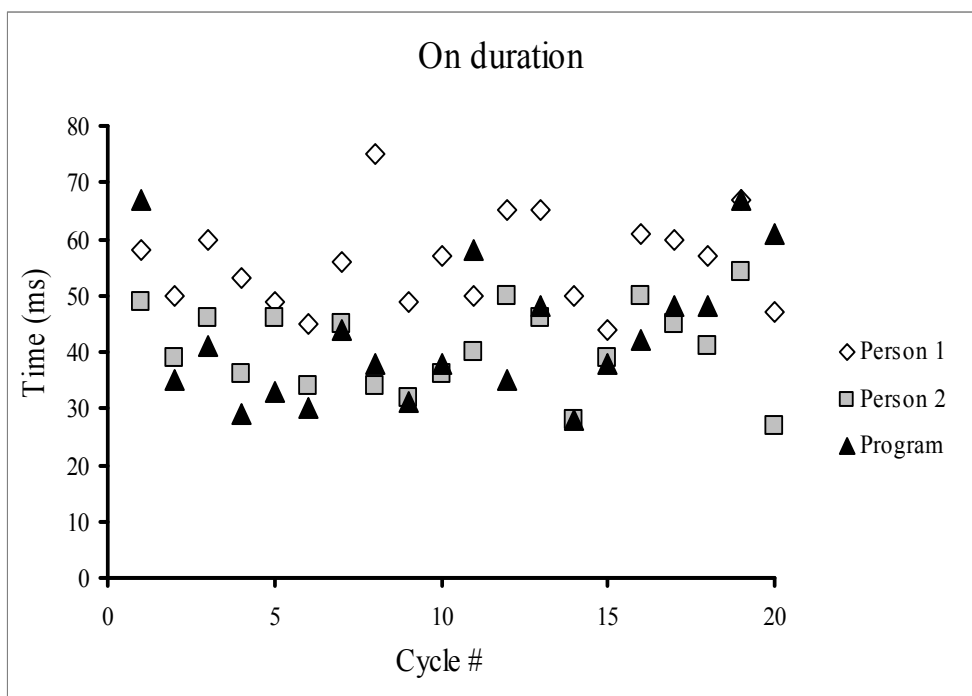


Fig. 5.7. Duration of EMG bursts measured by Person 1, Person 2 and the Program. The data were recorded from a spasm in the left medial gastrocnemius muscle during hour 8 (7-8 am; Subject C, injury at C6).

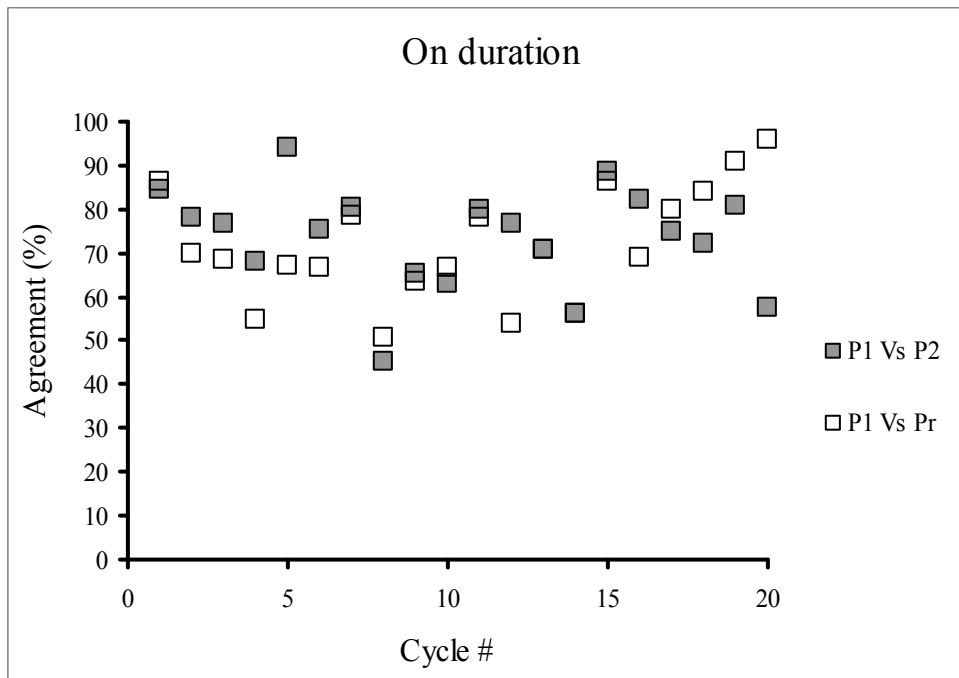


Fig. 5.8. Agreement for on duration between P1 and P2 and P1 and Pr. Data are for one clonus recorded from the left medial gastrocnemius muscle during hour 8 (7-8 am; Subject C, injury at C6).

Agreement for on durations On a subject-by-subject basis, agreement varied between 78-98% for the on durations of Person 1 and Person 2, and varied between 73-86% between Person 1 and the program. The average agreement for on durations was 85% (SE 3) between Person 1 and Person 2 and 77% (SE 2) between Person 1 and the Program (Fig. 5.9). An ICC coefficient of 0.905 was obtained when on durations were compared for Person 1 and Person 2 and a coefficient of 0.852 for Person1 and the Program. These values for intra-class correlation coefficients indicate good reliability of measurements. The differences in performance between Person 1 and between the operator and the program were not significant ($p=0.277$) indicating that the algorithm was as good as human operators at measuring the duration of EMG bursts during clonus.

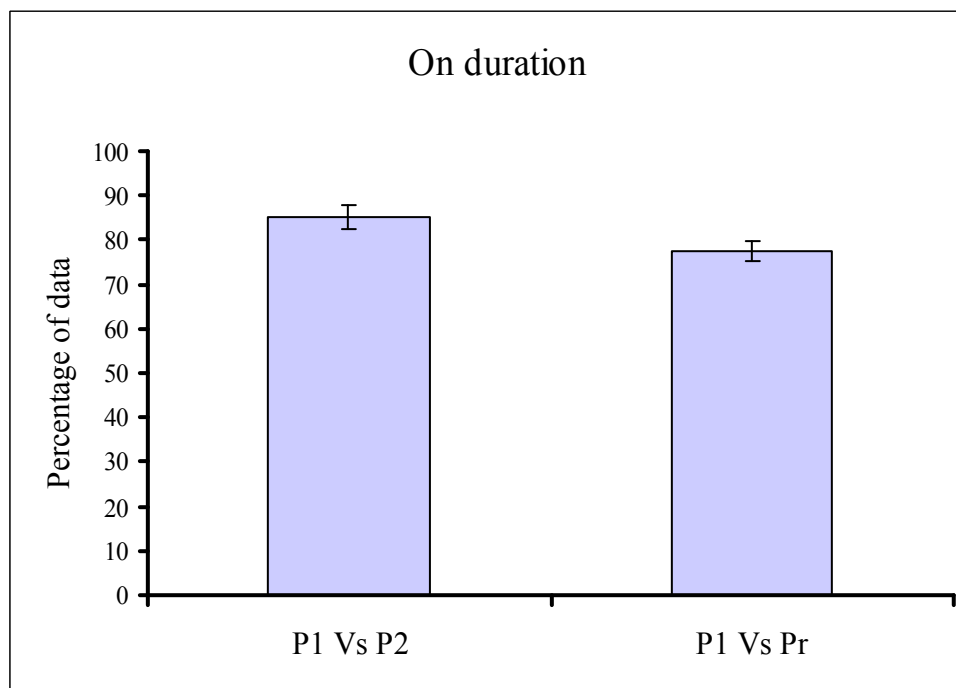
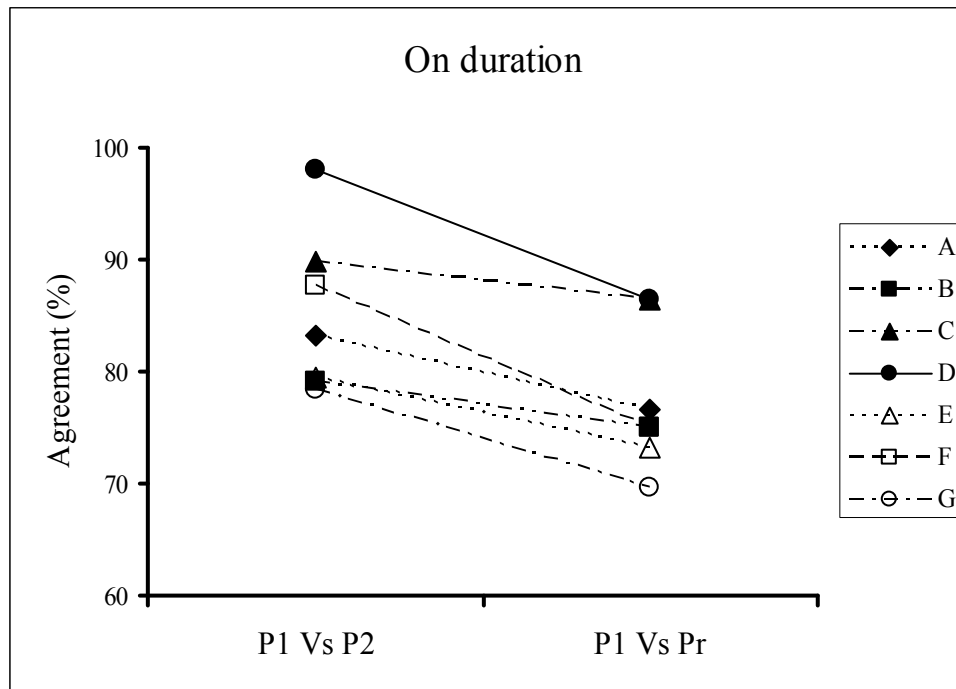


Fig. 5.9. Mean agreement for on durations for Person 1 and Person 2 and Person 1 and the program for each subject (top) and for group data (mean \pm SE; $n=7$; bottom).

Histograms that show the distribution of agreement for on durations measured by the operators and the program are shown in Fig. 5.10, where Person 1 and Person 2 agree to 90% on measured on durations for 46 % (± 11) of the data. The corresponding results for Person 1 and the program were 27% (± 6) of the data.

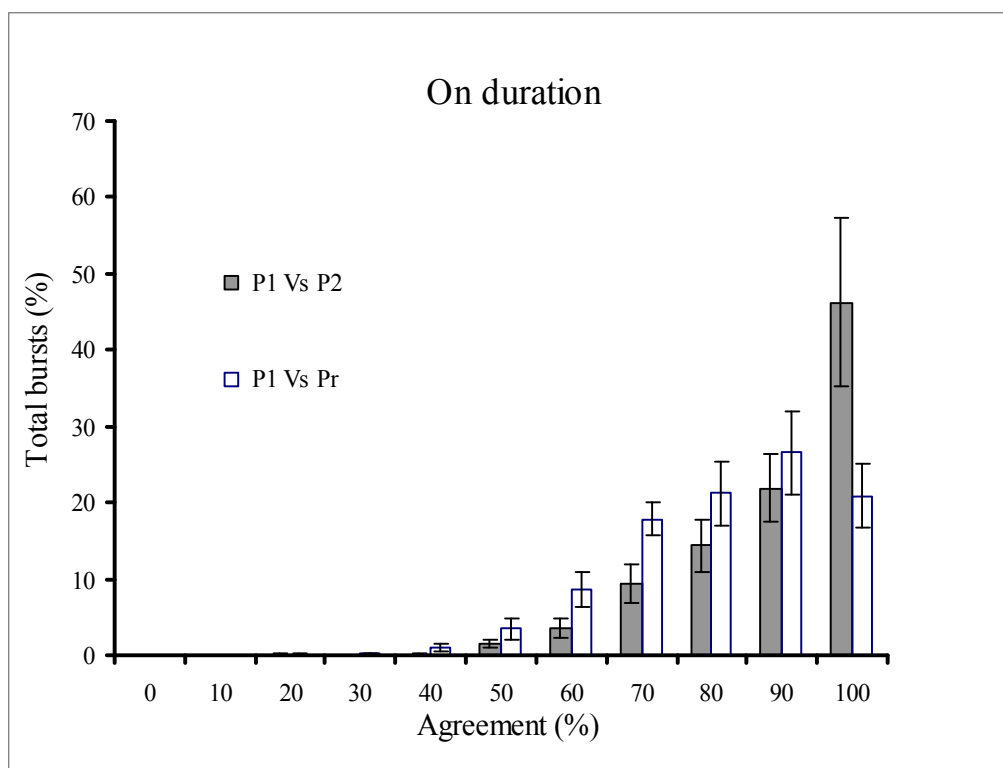


Fig. 5.10. The mean (\pm SE) percentage agreement for on duration between P1 and P2 and P1 and Pr ($n = 7$ subjects).

5.1.5 Clonus frequency

An important outcome of this analysis is the clonus frequency. The instantaneous clonus frequency was calculated from the start time measurements made for each spasm by both human operators and the program. A typical example of the clonus frequency obtained by the operators and the program is presented in Fig. 5.11. The average

frequency for this clonus was 8.3 Hz (± 0.9), 8.2 Hz (± 0.9) and 8.3 Hz (± 0.9) by Person 1, Person 2 and the Program, respectively.

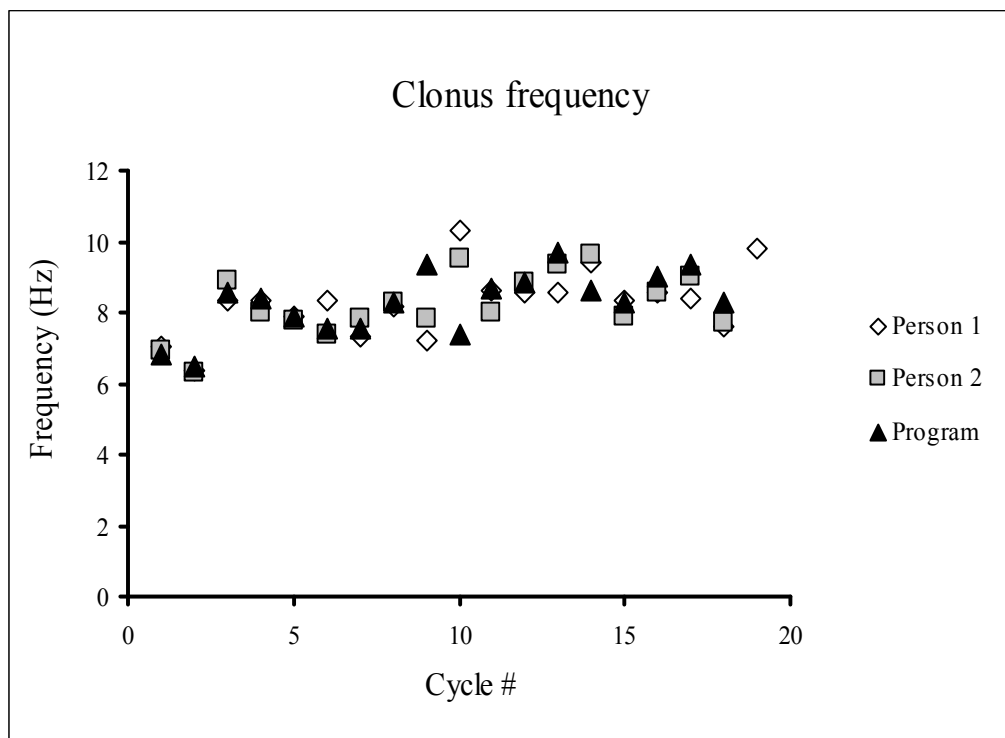


Fig. 5.11. Clonus frequency calculated from the markings made by the operators and the algorithm. The EMG were recorded from the left medial gastrocnemius muscle during hour 8 (7-8 am; Subject C, injury at C6).

Agreement on clonus frequency The average agreement for clonus frequency was 99.6 % (SE 0.2) between Person 1 and Person 2 and 99.4 % (SE 0.3) between Person 1 and the Program (Fig. 5.12). ICC coefficients for clonus frequency were 0.971 and 0.949 for Person 1 and Person 2 and Person 1 and the Program, respectively. These differences in clonus frequency for the operators versus Person 1 and the program were not statistically different ($p = 0.718$). Thus there was a high degree of reliability in

assessment of clonus frequency, support that the algorithm can determine clonus frequency reliably.

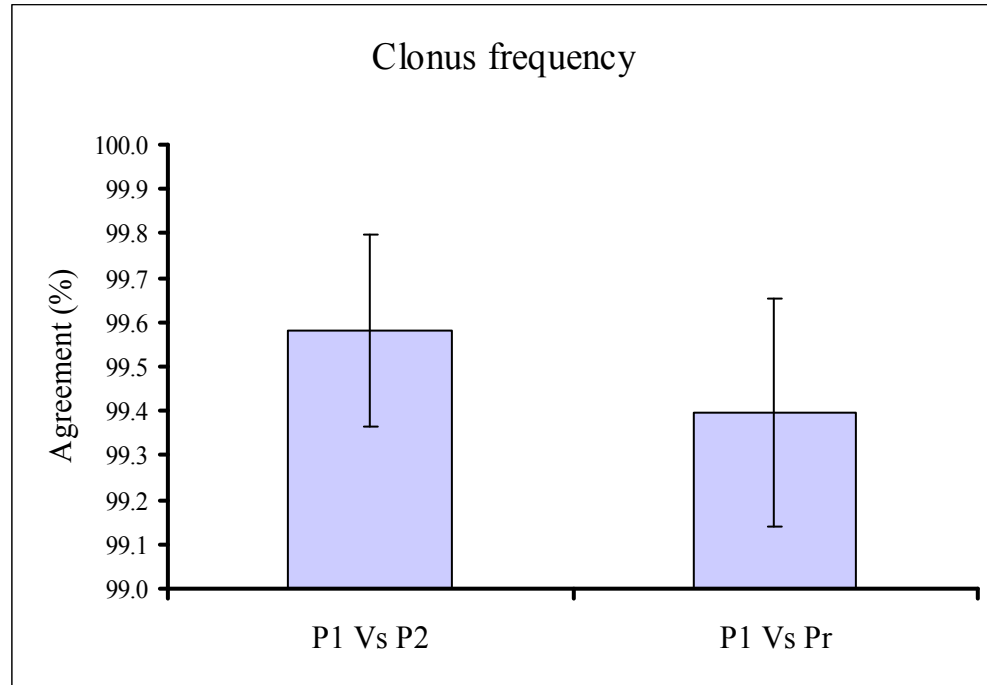


Fig. 5.12. Mean agreement on clonus frequency for Person 1 and Person 2 and Person 1 and the Program for the group data (n=7 subjects; mean \pm SE).

Differences in clonus frequency The mean percentage differences in clonus frequency for the operator(s) and the algorithm (Fig. 5.13) show that the percentage difference in clonus frequency varied by -2% to 2% for 60% of the data from Person 1 and Person 2 and for 51% of the data from Person 1 and the Program, indicating a close match between both the measurements. A 2% change results in a difference of 0.06 to 0.12 Hz in clonus frequency that ranges from 3-8 Hz.

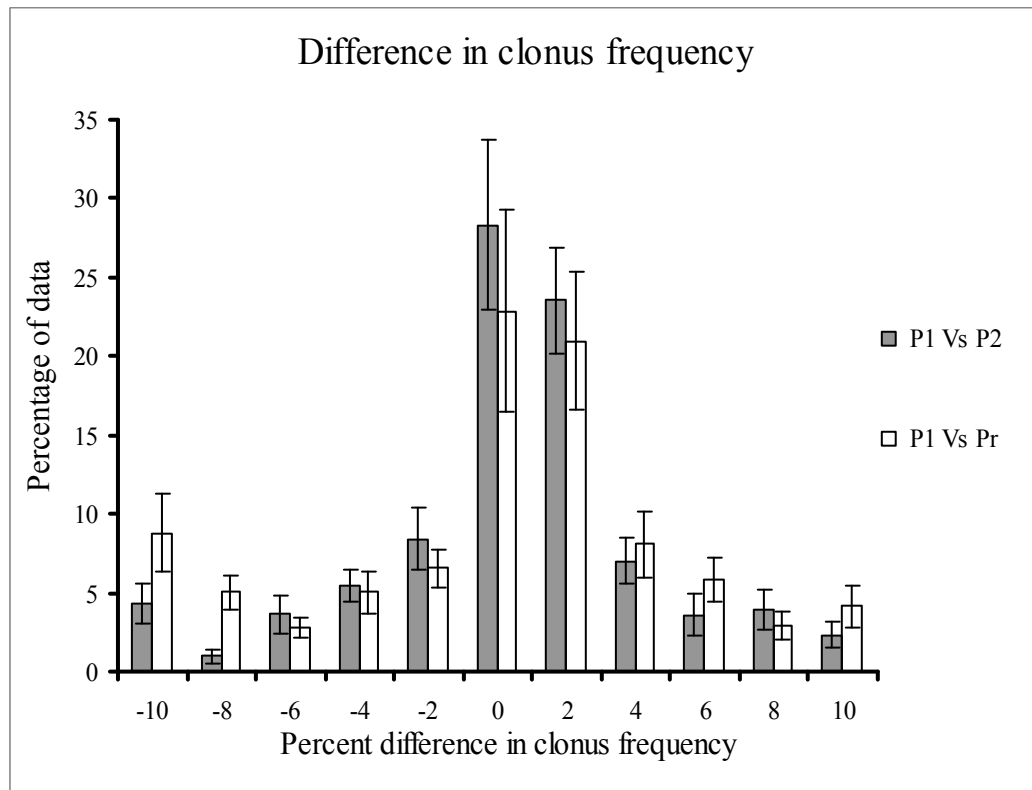


Fig. 5.13. Average (\pm SE) difference in clonus frequency for P1 and P2 and P1 and Pr (n=7 subjects; n=31 spasms).

Constraints on the algorithm increased the accuracy of detecting EMG bursts and determining clonus frequency Clonus frequency relies on detecting the EMG bursts accurately, which was improved by constraints imposed on the algorithm. In the algorithm that detects the start and the end of the EMG bursts, two sets of constraints were applied to improve performance.

- 1a. An intensity threshold ($25\mu V^2$) was used to eliminate peaks arising from baseline noise.
- 1b. A time constraint between adjacent peaks was implemented to avoid multiple peaks due to EMG changes.

2a. The window was resized on either side of the detected EMG burst to determine the start and the end of the EMG and to eliminate motor units firing between the bursts. 2b. An energy threshold (7.5 mV^2) was used to eliminate motor unit potentials at the beginning or the end of clonus.

To understand the effects that these constraints had on the number of EMG bursts identified, the results without and with constraints were compared. For example the data from subject A (Fig. 5.14) show that the first set of constraints played a crucial role in reducing the false detection of EMG bursts and bringing the number of bursts identified closer to the human judgement. The second set of constraints mainly eliminated the motor units from being marked as EMG bursts.

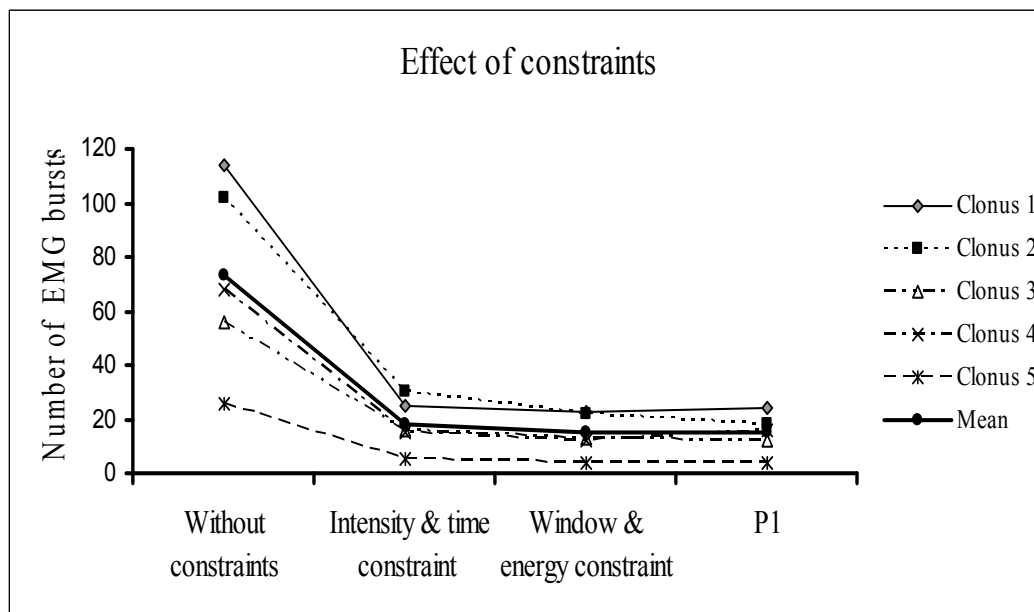


Fig. 5.14. Number of EMG bursts identified without any constraints and with the addition of each set of constraints compared to the bursts identified by Person 1. The EMG data were collected from subject A (injury at C6).

A similar trend was observed for all 7 subjects in this study (Fig. 5.15). An average of 730 % (SE 117) more EMG bursts were identified by the program without any constraints, compared to that by Person 1. Introduction of the first set of constraints reduced the false detection of bursts to 133% (SE 10) of that marked by Person 1. Implementation of the second set of constraints brought the number of peaks to 99% (SE 2) of Person 1 (100% denotes the exact number of peaks identified by Person 1). One way ANOVA of ranks on the bursts identified by the program and the Person 1 without and with each set of constraints were calculated. There was a significant reduction in the number of EMG bursts identified by the algorithm without any constraints versus after applying the first set of constraints ($p \leq 0.001$). The differences between the results of the constrained algorithm and Person 1 were not statistically different. That is, the EMG bursts detected by the program closely matched that of Person 1 suggesting that the first set of constraints was crucial in reducing erroneous peaks.

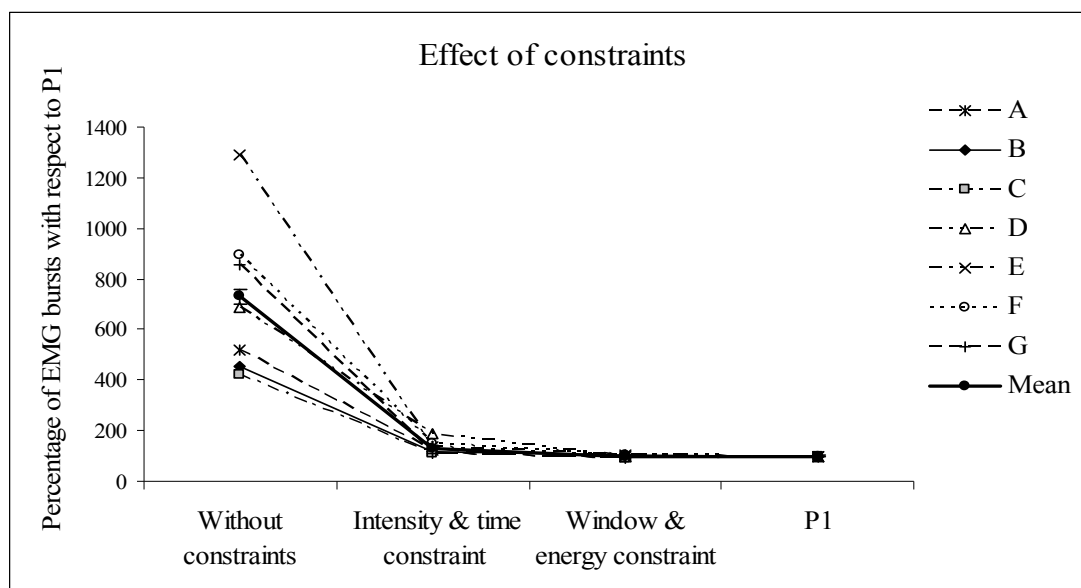


Fig. 5.15. EMG bursts detected by the algorithm with and without constraints as compared to Person 1 (n=7 subjects; n=31 spasms).

The mean agreement between the number of EMG bursts detected by Person 1 and the algorithm is shown for each subject in Fig. 5.16. The agreement for subjects C and G was 90% and 91% largely due to several motor unit potentials firing between the EMG bursts making the silent period unclear. For subjects B, E and F the agreement was greater than 100 %, which was due to the algorithm identifying motor unit potentials as peaks and so more peaks than Person 1.

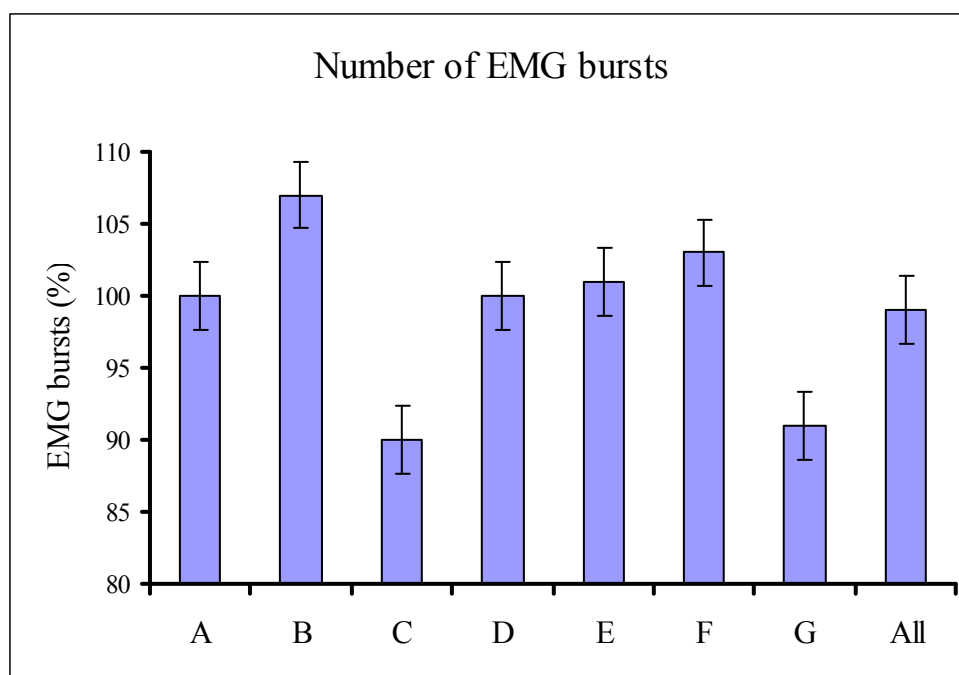


Fig. 5.16. Mean agreement (\pm SE) for the number of EMG bursts identified by Person 1 and the Program by subject (A-G) and for 7 subjects (All).

5.1.6 Intensity of contractions

The RMS value of each burst of EMG during clonus was calculated from the start and the end times and used to indicate the intensity of the contractions during

clonus. A typical example of RMS values obtained from one clonus (Fig. 5.17) shows high agreement between operators and the program.

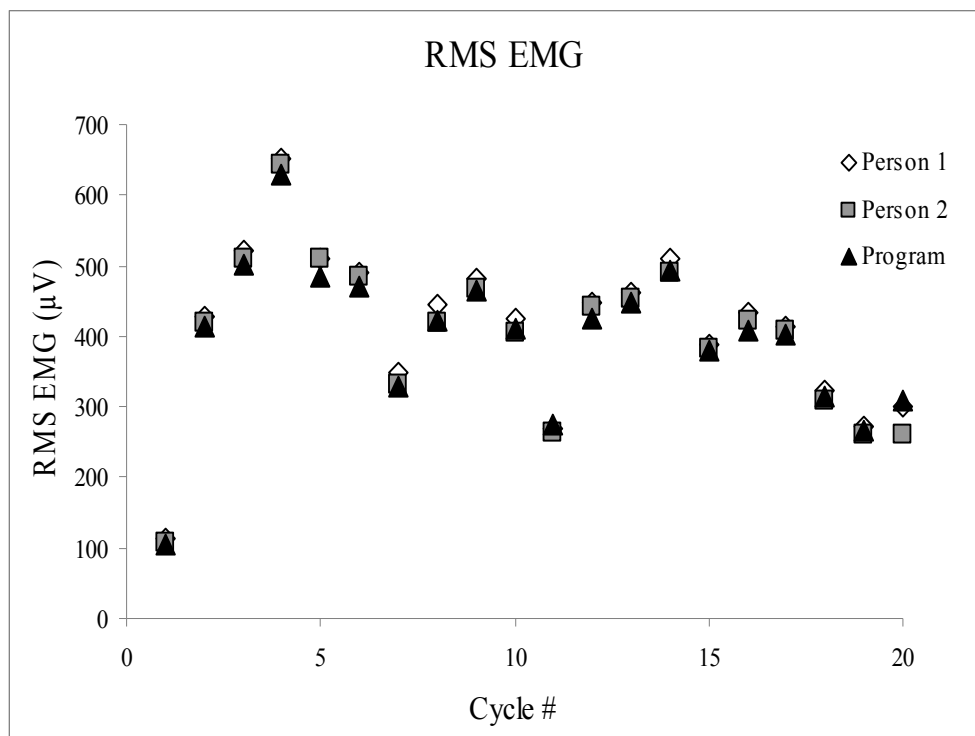


Fig. 5.17. RMS values for each EMG burst in one clonus. The EMG were recorded from the left medial gastrocnemius muscle during hour 8 (7-8 am; Subject C, injury at C6).

Agreement on RMS values for EMG bursts Agreement averaged 98.8 % (SE 0.3) between Person 1 and Person 2 and 97.4 % (SE 0.5) between Person 1 and Program for the RMS value of the EMG bursts during clonus (Fig. 5.18). An ICC coefficient of 0.997 was obtained for the two operators and between Person 1 and the Program indicating good reliability in assessment of RMS values during clonus. As the coefficients were the same, the Program is as reliable as human operators in measuring the intensity of contractions during clonus.

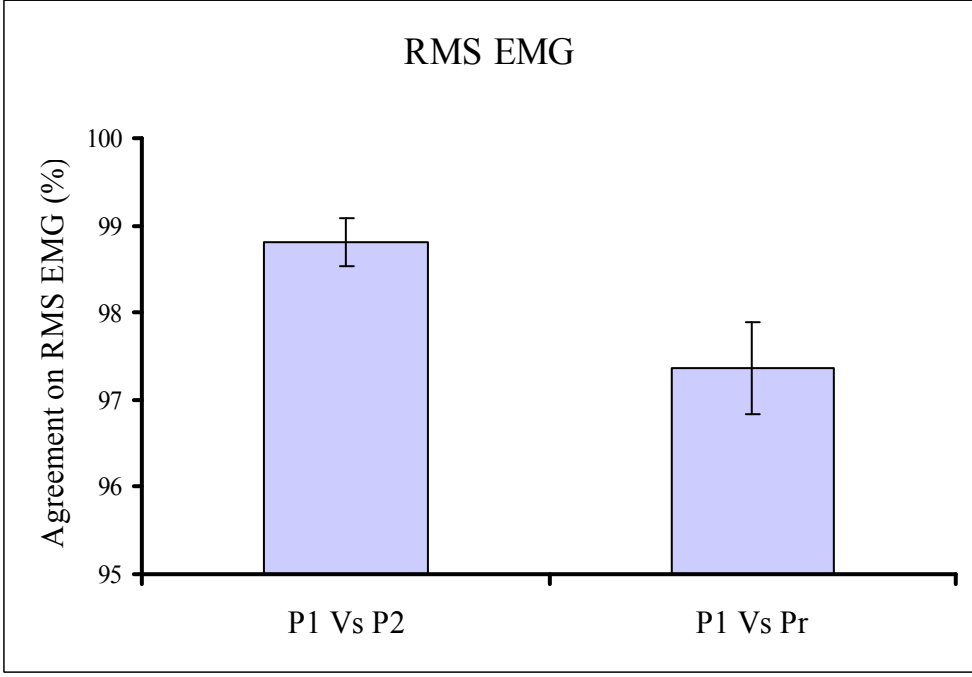
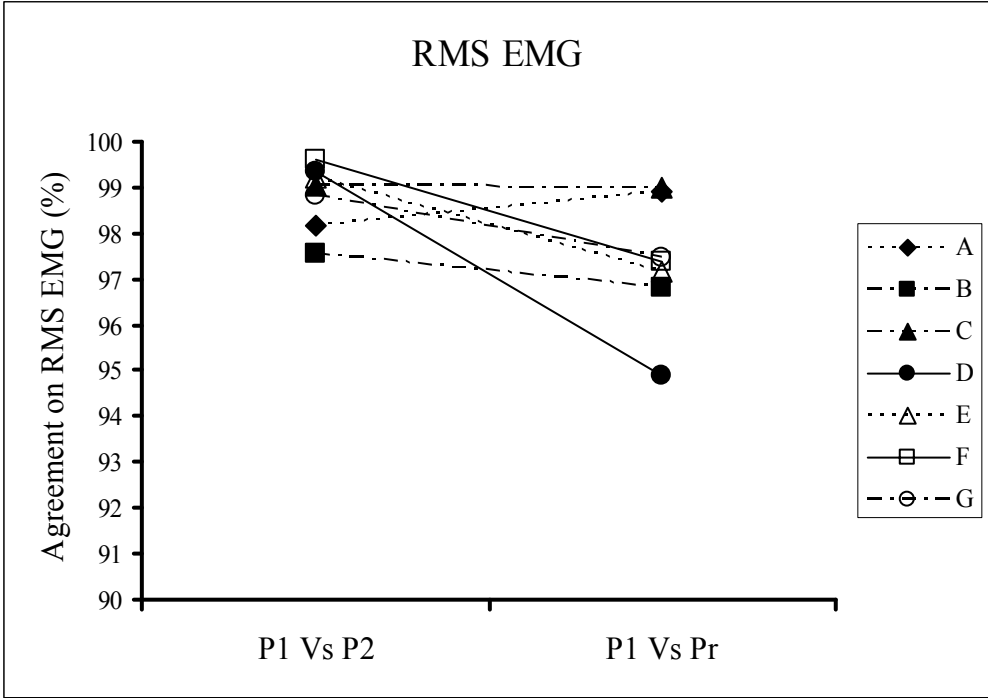


Fig. 5.18. Average agreement on RMS values for EMG bursts assessed by Person 1 and Person 2 versus Person 1 and the Program by subject (top) and group (mean ± SE; n=7 subjects; bottom).

Differences in RMS values for EMG bursts The average (\pm SE) difference in RMS values between operator(s) and between Person 1 and the algorithm were mostly distributed within a -2% to 2% difference. Most of the data from Person 1 and Person 2 (73%) and 44% of the data from Person 1 and the Program fell within the -2% to 2% bins (Fig. 5.19). The distribution of differences in RMS values is skewed towards the left for the comparison between Person 1 and the Program versus Person 1 and Person 2 results due to consistently shorter on durations from the Program compared to Person 1. However given the magnitude of the maximal EMG during some contractions involving clonus (650 μ V in Fig. 5.17), a \pm 2% difference in RMS is small.

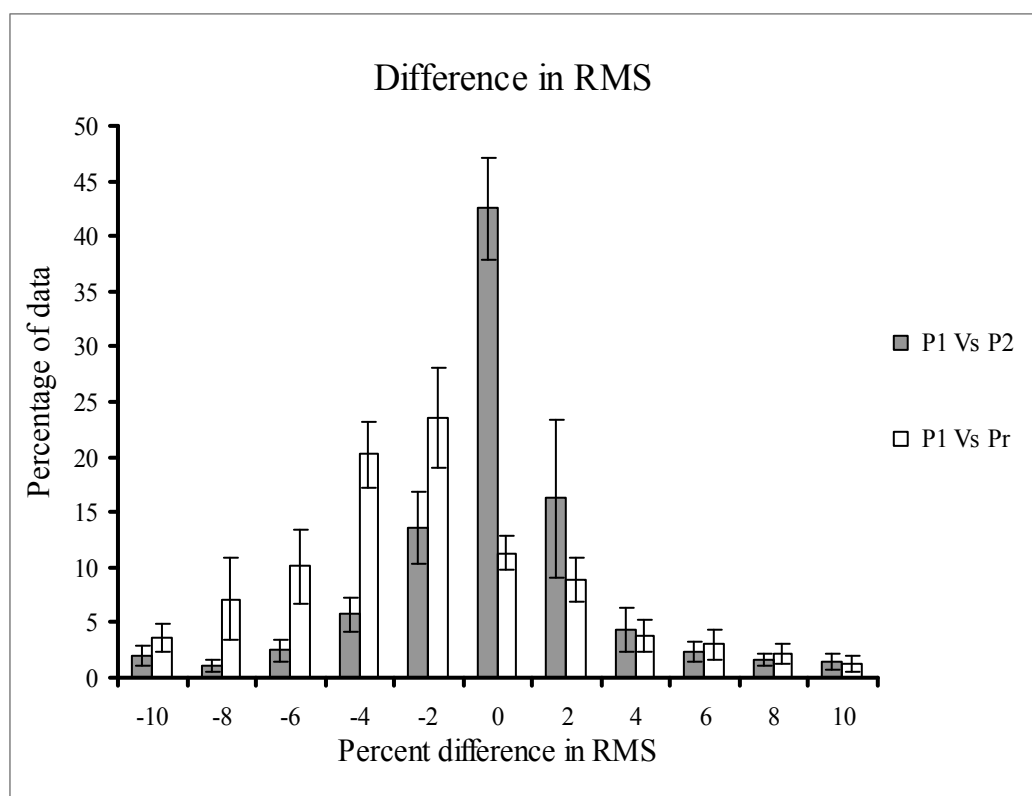


Fig. 5.19. Average (\pm SE) difference in RMS values obtained for Person 1 and Person 2 and Person 1 and the Program (n=7 subjects).

5.1.7 Measurement time

The time taken to view and mark the start and the end times of the EMG bursts for each spasm was recorded for each operator and the algorithm. The algorithm was significantly faster at analysis than both of the human operators ($p \leq 0.001$), who took a similar time to measure the clonus ($p \geq 0.05$). For example, to measure the start and end times of EMG in clonus that lasted 10 s took 1440 s (24 minutes) for Person 1, 3180 s (53 minutes) for Person 2 and 1.64 s for the program. To measure all 31 spasms it took 6 hours for Person 1, 13 hours for Person 2 and 1.15 minutes for the algorithm. Thus for the group data ($n = 31$ spasms), the program was 336 (SE 46) times faster than Person 1 and 813 (SE 117) times faster than Person 2. These results indicate the efficiency of this novel algorithm.

5.2 Analysis of clonus in a single muscle over 24 hours

The algorithm developed was as good as a human operator at analysis of clonus. To test the ability of the algorithm to analyze clonus from long-term recordings, 24 hours of data from the right medial gastrocnemius muscle from subject F were analyzed. A total of 73 spasms involving clonus were identified by the experts in the entire 24 hour recording. The algorithm analyzed all of these spasms and produced text file outputs for each spasm in 8 minutes. The output was visually observed using Dadisp software and corrected for discrepancies in 4.3 hours. The estimated time to perform the 24 hr analysis manually was 17.9 hours. The output files were transferred into an Excel template to calculate on duration, clonus frequency and the RMS value of EMG during each burst of clonus. The analysis was divided into clonus during sleep (hours 1- 8; $n = 6$ spasms; 8%

of the 73 spasms with clonus) and awake time (hours 9 - 24; n = 67 spasms). Clonus was more prevalent in awake hours than during sleep time. During the 24 hours, there was no clonus during 3 sleep hours and 2 hours of awake time.

5.2.1 Number of EMG bursts during clonus

The mean number of EMG bursts during clonus over 24 hours was 27 (SE 4; range 3 - 215 bursts). On average clonus lasted for 9.1s (SE 1.3; range 0.9 - 92.0 s). Clonus was shorter during sleep than during awake time (fewer bursts of EMG). Clonus involved an average of 18 (SE 4) bursts of EMG during sleep and 28 bursts (SE 4) during the awake period (Fig. 5.20). However the sleep-awake difference was not statistically significant ($p=0.488$).

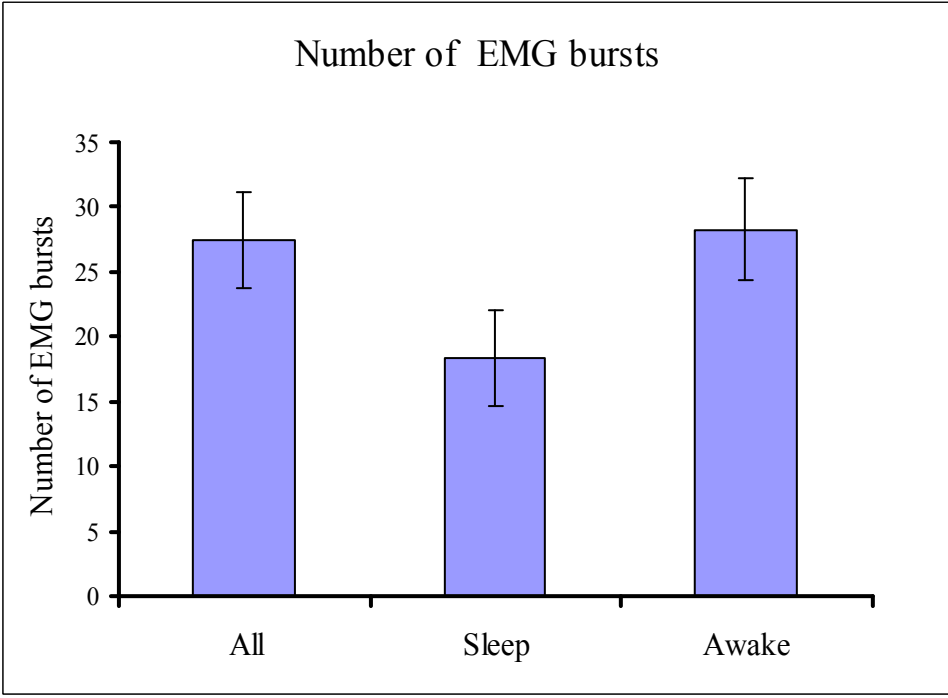
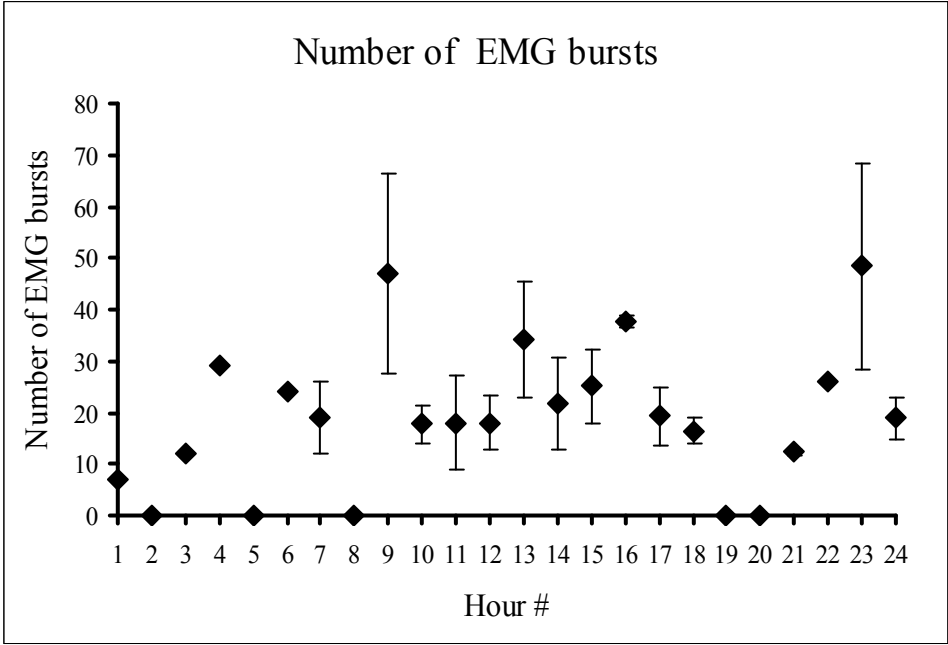


Fig. 5.20. Mean (\pm SE) number of EMG bursts during clonus in 24 hours (bottom), and that during sleep (hours 1 - 8) and awake periods (hours 9 - 24) by hour (top; hour 1 = Midnight to 1 am).

5.2.2 On duration

The duration of EMG bursts averaged 47 ms (SE 1, range 34-80 ms) during the 24 hour recording (Fig. 5.21). The duration of the EMG bursts did not change significantly ($p = 0.077$) when clonus occurred during sleep (mean 53 ms; SE 4; range 44-71 ms) versus awake time (mean 47 ms; SE 1; range 34-80 ms). The duration of EMG bursts was relatively consistent during the entire 24 hour recording.

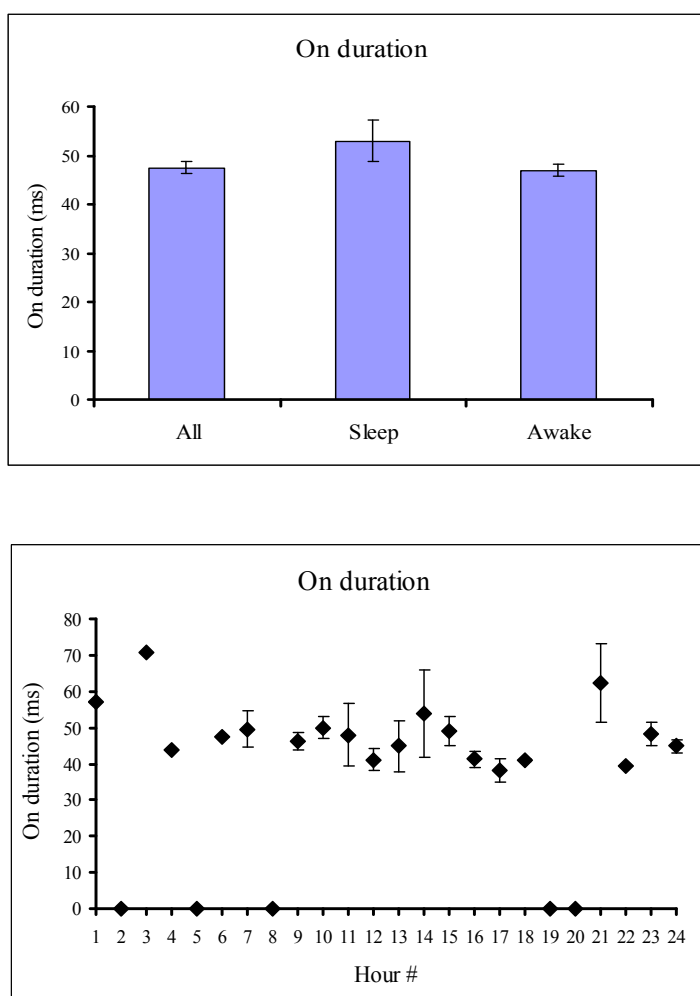


Fig. 5.21. Mean (\pm SE) EMG burst duration in 24 hours, during sleep and awake periods (top) and by hour (bottom).

5.2.3 Clonus frequency

The mean clonus frequency over 24 hours was 6.3 Hz (SE 0.1; range 4-9 Hz, Fig. 5.22). Clonus frequency was not significantly different ($p=0.192$) between sleep (mean 5.9 Hz; SE 0.22) and awake hours (mean 6.3 Hz; SE 0.13).

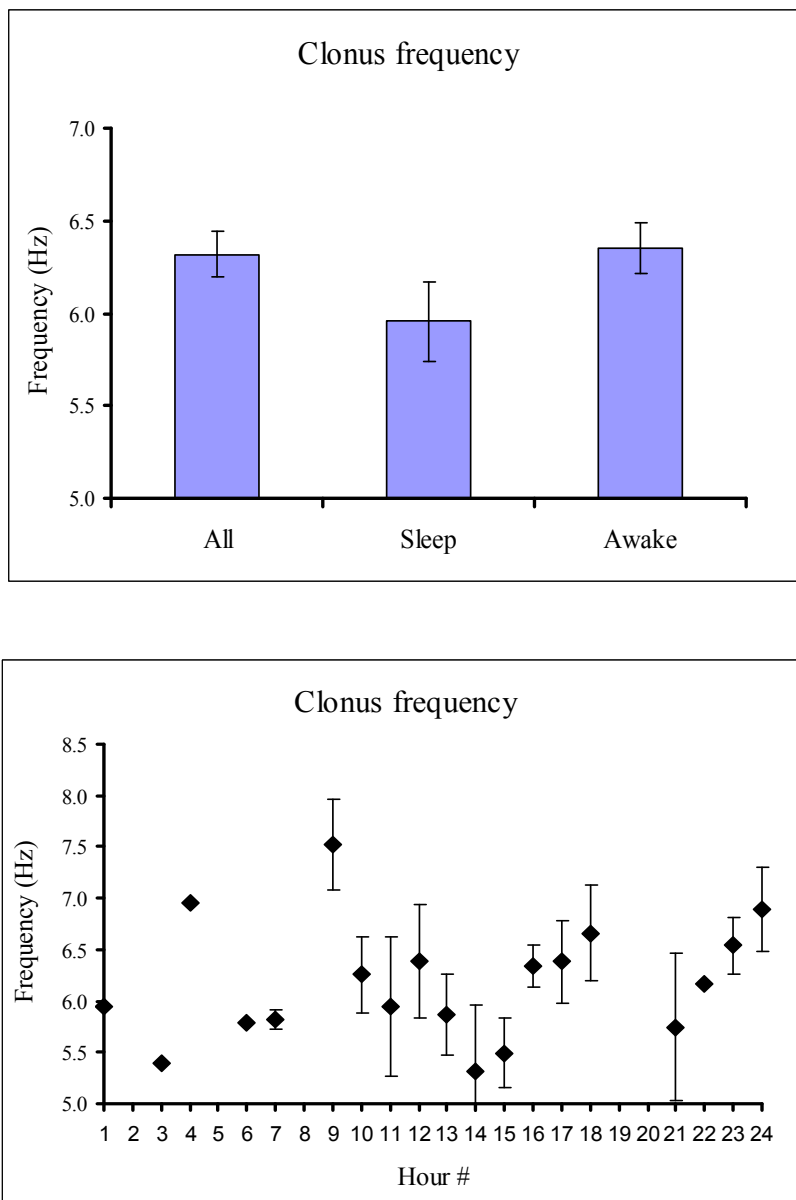


Fig. 5.22. Mean (\pm SE) clonus frequency in 24 hours, during sleep and awake periods (top) and by hour (bottom; $n=73$ spasms).

5.2.4 Intensity of contractions

Over 24 hours the mean RMS EMG, a measure of contraction strength, was 331 μV (SE 27; range 37- 953 μV) (Fig. 5.23). The average RMS value of the EMG bursts was significantly lower ($p = 0.038$) during sleep (mean 145 μV ; SE 39; range 38 - 255 μV) than during awake time (mean 348 μV ; SE 28; range 37- 953 μV). To estimate the strength of the contractions during clonus, the average RMS EMG was normalized to the maximal M-wave for that muscle. Since the clonus involves asynchronous motor unit activity but the M-wave is a synchronous response the normalized RMS EMG were adjusted using able bodied data (the ratio of the M-wave amplitude to the amplitude of maximum voluntary contraction which was 5). Estimated this way, contractions during clonus were 53% maximal during awake time and 23% maximal during sleep time, on average. Thus, clonus involves strong contractions and particularly during awake hours.

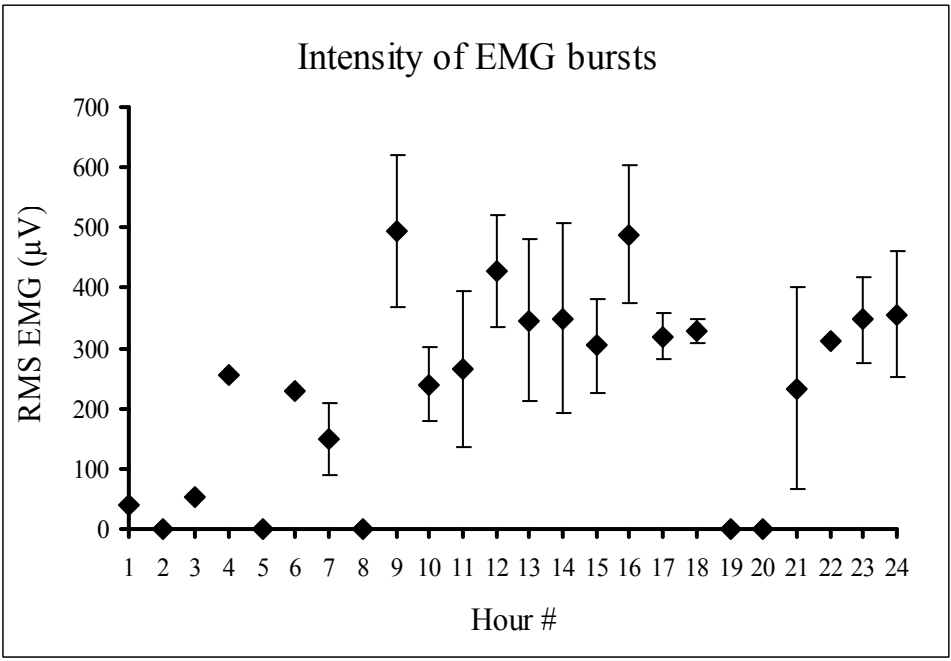
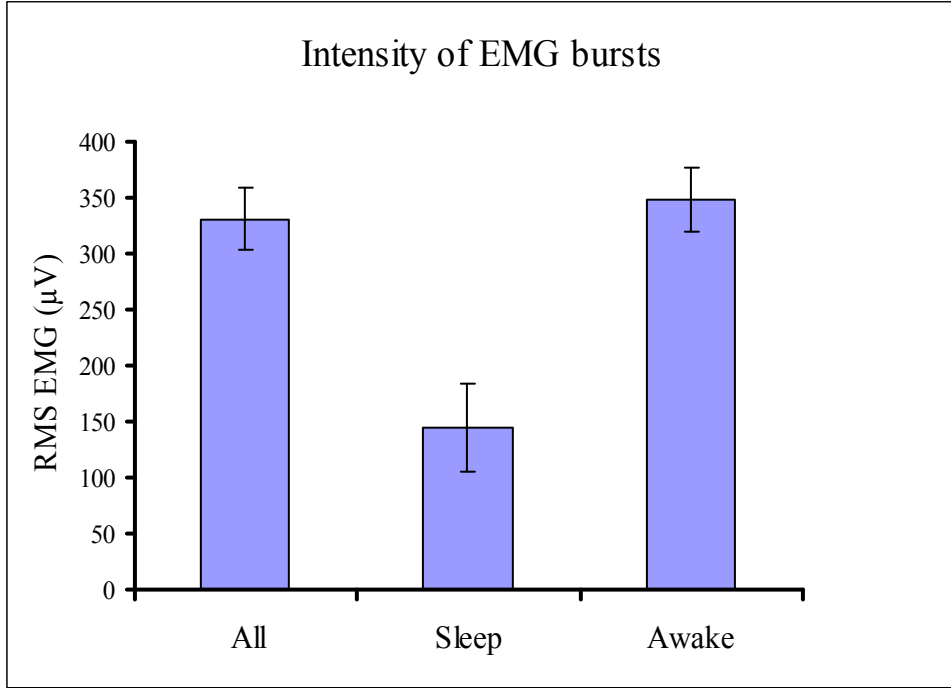


Fig. 5.23. Mean (\pm SE) RMS EMG during clonus in 24 hours, during sleep and awake periods (top) and by hour (bottom; $n = 73$ spasms).

5.2.5 Changes in parameters during clonus

The durations of different spasms involving clonus differ markedly (range: 0.9 – 92.0 s). To understand the variations in on duration, clonus frequency and intensity these data were expressed independently of the duration of clonus. The beginning and end of clonus was assigned values of 0% and 100% relative time, respectively. The duration of EMG bursts decreased during clonus that occurred during either sleep or awake time. although these changes in the duration of EMG bursts were not statistically significant ($p= 0.694$).

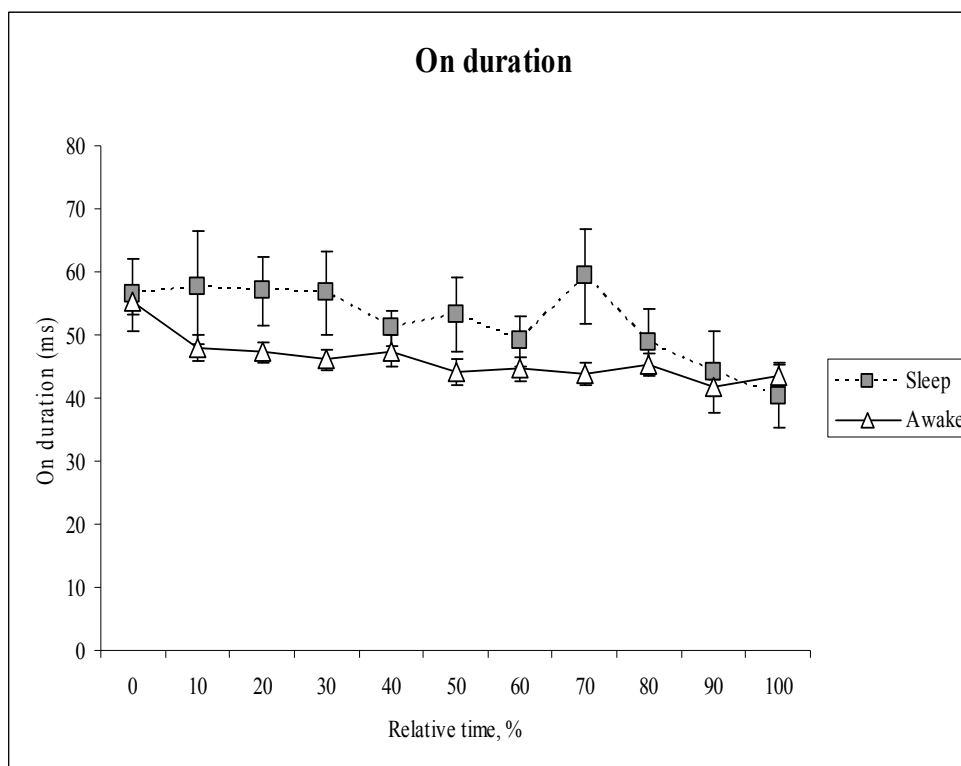


Fig. 5.24. Average (\pm SE) duration of EMG bursts in 24 hours separated by sleep and wake periods and represented independent of clonus duration ($n = 8$ and 65 spasms, respectively).

The average clonus frequency was relatively similar throughout the clonus during both sleep and awake periods (Fig. 5.25).

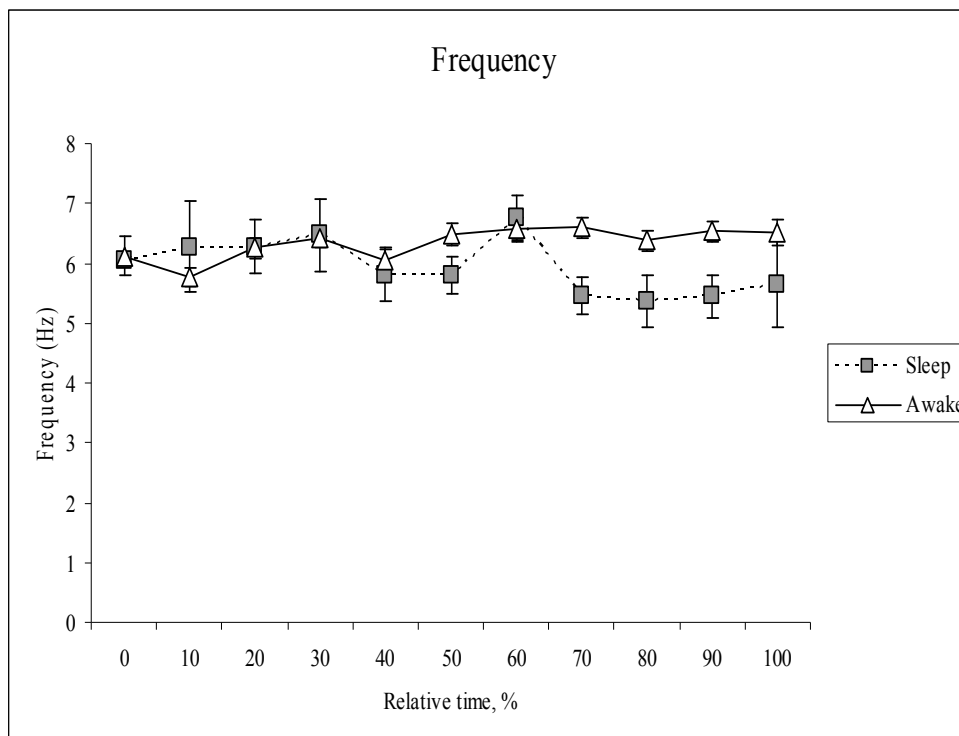


Fig. 5.25. Average (\pm SE) clonus frequency in 24 hours during sleep and awake periods and represented independent of clonus duration ($n = 8$ and 65 spasms respectively).

During sleep the contractions increase in intensity up to 20% of total clonus duration then gradually decrease towards the end of clonus. A similar trend was found for clonus during awake time, but the intensity increased up to 60% of total clonus duration, indicating that the strong contractions were sustained for a longer relative time (Fig. 5.26). However these changes in contraction intensity during both sleep and awake times are found to be statistically insignificant ($p = 0.941$).

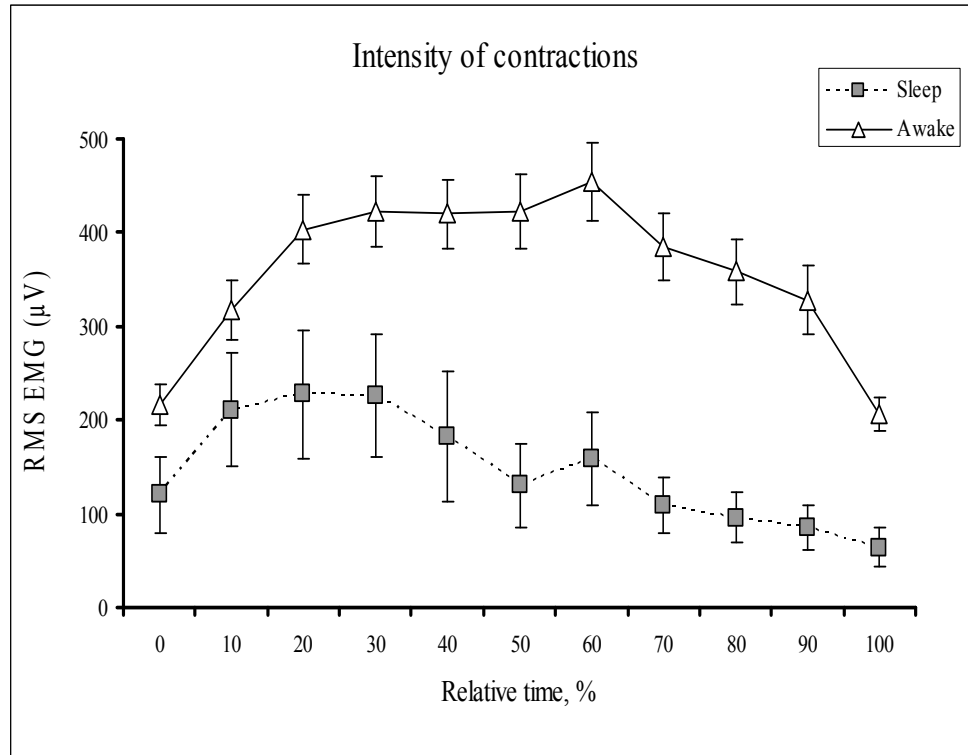


Fig. 5.26. Average (\pm SE) RMS EMG of bursts during clonus in 24 hours during sleep and wake periods and represented independent of clonus duration ($n = 8$ and 65 spasms, respectively).

Chapter 6: Discussion

The algorithm developed in this study was able to automatically determine the location of EMG bursts, the duration of EMG bursts, clonus frequency, and the intensity of each EMG burst during clonus. The algorithm was as accurate as two human operators in measuring these parameters, support for the first hypothesis. The agreement between a person and the program was highest for clonus frequency, followed by the EMG intensity then the duration of EMG bursts. Efficient detection of the EMG bursts and the peak EMG, which was refined by imposing constraints on the algorithm, was key to accurate measures of clonus frequency and intensity.

6.1 Detection of bursts of EMG during clonus

Clonus involves rhythmic and repetitive muscle contractions resulting in bursts of EMG separated by relative silent periods (Walsh 1976, Dimitrijevic et al. 1980, Rack et al. 1984). The identification of EMG bursts during clonus is of crucial importance from a clinical stand point of view. The number of bursts of EMG convey information about clonus duration. A longer spasm may be more disruptive and make it more difficult to perform daily activities (Little et al. 1989, Sheean 2002, Adams and Hicks 2005).

The algorithm developed here used intensity analysis (Von Tscherner 2000) to envelope the EMG in different frequency bands. Time and frequency aspects of the EMG are considered simultaneously, a process that is not achieved by conventional analysis of EMG. The intermediate frequency band envelope (80-190 Hz) best fit the EMG bursts during clonus as the physiological frequencies of surface EMG largely falls in this band.

But EMG during clonus involves asynchronous activity of motor units and the potentials fuse to cause multiple peaks in the EMG. The intermediate frequency envelope obtained from intensity analysis still had multiple peaks for each burst of EMG but the algorithm needed to identify only one peak for each burst of EMG so start and end times could be measured for every cycle of clonus. Thus constraints (intensity threshold and time constraints) were imposed on the algorithm to help achieve this. The intensity threshold eventually discarded peaks caused by baseline fluctuations whereas a time constraint of 90 ms, the minimum time separation between two adjacent peaks, was optimal for the majority of experimental data, consistent with observations that clonus frequency rarely exceeds 10 Hz in leg muscles of adults (Dimitrijevic et al. 1980, Wallace et al. 2005). However in some cases motor units were prevalent between EMG bursts. To avoid false detection of peaks from these motor units, the low frequency envelope was used to detect the EMG peaks. Since motor unit potentials have higher frequency components and their effects are less pronounced in the low frequency band, this conditional choice of frequency band refined the EMG peak detection. The constrained algorithm was tested with data from 7 different experiments and at least 2 leg muscles per recording (except for subject D). In all cases, the output was as reproducible as the results of a person. The rhythmic nature of clonus and the predictable pattern of EMG during clonus also facilitate this success.

6.2 Measurement of the start and the end of the EMG burst

The start and end times of EMG bursts were determined by finding where the energy contained in a window region around the EMG peak reached 5 % and 95 % of the maximal value respectively. Motor unit potentials that fired in between the bursts because

of their early or late response to the muscle stretch (Wallace et al. 2005) were not part of the EMG burst but fell within the windows. To eliminate these motor unit potentials the windows were resized to 50 ms on either side of each identified EMG peak. This 50 ms duration criterion was based on data from subjects A and F, where the motor units typically fired 60-80 ms before the EMG burst. Resizing the window had no impact on detecting the start and end times of the EMG burst because the burst durations averaged 47 ms (SE 1) in the 24 hour analysis carried out in this study, results that are consistent with reported ranges of 40 -70 ms (Dimitrijevic et al. 1980, Wallace et al. 2005). However when motor unit potentials do fall within the resized window they are included in the energy calculation used to determine start and end times. The differences in start and end times measured by Person 1 and the Program were close to 10 ms (Fig. 5.2). Potentials that fall within the 5-95% of energy values will be included which may add 10 ms to the start and/or end time, a typical duration for a motor unit potential (Thomas et al. 2006). In contrast a potential smaller than 5% of the total energy will be excluded. Thus, the chance of inappropriate inclusion of a motor unit potential is higher when the intensity of the EMG burst is low.

Discrepancies between the start and the end times measured by human operators or a person and the program (differences ≥ 25 ms) were largely caused by either including or excluding motor unit potentials, the presence of slow waves from filtering the data, big potentials, and EMG activity between bursts. In addition to the motor unit potentials near the start and end of bursts of EMG, big potentials sometimes occurred in the EMG bursts possibly due to unit synchronization. In these cases the program starts and ends the burst early because the majority of the energy is contributed by the big

potential alone resulting in shorter burst durations. The after effects of filters, slow waves, were included by Person 1 but excluded by the program because they did not meet the 5-95% energy criteria for defining the start and end times. These filters did eliminate other noise and artefacts from the 24 hour EMG records, however. Other discrepancies in start and end times were caused by inter-burst EMG activity in marking the onset of the bursts unclear. This same issue also resulted in detection of additional bursts of EMG during clonus by the person or the program as did tonic EMG and motor unit potentials at the start and end of the spasms involving clonus.

Overall, start and end times influence both the duration and the intensity (RMS) of the EMG bursts. The algorithm was accurate at measuring the on duration of EMG bursts for the reasons already described. Even on durations measured by people were relatively constant across spasms and experiments because of the timing of the peripheral input to the spinal cord is relatively reproducible.

Contractions intensity during clonus has not been evaluated in any previous studies involving clonus. However the RMS EMG was important to measure because it can be used to describe the severity of contractions. Strong contractions may be more disruptive to the person. Documenting clonus contraction intensities could help in designing interventions to mitigate clonus. The algorithm was as good as a human operator at determining the intensity of the contractions from the detected start and end times of the EMG bursts because of the energy contributed by a 10 ms discrepancy is small. Good estimations of changes in EMG intensity have also been made during running, and during fatiguing exercise on a cycle ergometer (Von Tscharnner 2002, Von Tscharnner et al. 2003).

6.3 Analysis time

The algorithm was 574 times faster than human operators at locating and measuring the start and end times of EMG bursts during clonus, results that support the second hypothesis of this study. An algorithm that is accurate and fast is invaluable for processing large volumes of data. Even though a person still needs to visually verify the output produced by the algorithm when analyzing 24 hour records, particularly with respect to false identification of tonic EMG and motor unit action potentials as clonus, the time needed to correct outliers is still approximately 4-5 times less than manual analysis alone. Moreover, human operators measure optimally when the clonus duration is short. To measure spasms of long duration (>10 s), a person has to be consistent in their measurements and decision making. This task requires concentration. Otherwise mistakes are made. Completing this analysis on a regular basis is also laborious and uninteresting. Thus it is ideal to automate such labor intensive processes to maximize accurate data analysis.

6.4 Characterization of clonus

By analyzing clonus in one medial gastrocnemius muscle over 24 hours it is clear that clonus was more prevalent during awake periods (92% of the spasms) than during sleep. The number of EMG bursts (hence clonus duration), clonus frequency, and contraction intensity were all higher during awake versus sleep time although only intensity was significant. The average intensity of clonus during awake period was found to be 53 % of the maximal muscle response indicating the high strength of contractions during clonus. Since inputs from the periphery to leg muscles are more likely when a

person is awake, external stimuli probably induced the more frequent and stronger clonus. If so, these results provide further support for the idea that clonus is driven by reflex mechanisms, as suggested by others (Cook 1967, Iansek 1984, Rack et al. 1984, Hidler and Rymer 2000).

Normalizing the data by time to eliminate differences in clonus duration across spasms demonstrated that the duration of the EMG bursts declined during the spasm while and the clonus frequency remained almost constant throughout the clonus. Both parameters usually decrease at the start and end of the spasm but these effects are dampened when averages are made, particularly when long duration clonus is included. In contrast, the intensity and number of bursts (overall clonus duration) varied more between awake and sleep periods suggesting that the strength of contractions and their number may be more crucial in determining what a person considers is severe clonus. These are also the parameters that could be targeted by interventions to reduce the disruptions caused by involuntary contractions. Since earlier studies on clonus were essentially done on the steady state period of clonus, and in standard laboratory settings for short durations of time (Walsh 1976, Dimitrijevic et al. 1980, Iansek 1984, Rack et al. 1984, Rossi 1990, Jones et al. 2003), the variations reported here for clonus strength and prevalence are novel findings.

6.5 Limitations and future developments

Even though a fair degree of automation was achieved by the algorithm, it still seeks human assistance for better performance. The algorithm works best when clonus occurs alone. It is less optimal when clonus is amongst tonic EMG and motor unit

potentials. In these situations user intervention is critical for accuracy. The accuracy can be improved by manually correcting the output files with assistance from the user interfaces developed here. Even with the manual corrections, the time invested for accurate analysis is still much less than required with complete manual analysis. The algorithm was able to successfully process and analyze data in minutes and correction took a few hours. This same analysis could take days of work hours if done manually.

Currently there are no existing methods reported to analyze clonus automatically from long term (24 hr) recordings. The algorithm developed in this study is one possible approach to this labor intensive task. Future research could enhance automation. For example, thresholds for intensity and motor unit potentials could be adapted depending on the complexity of EMG. Identification of where there the clonus is in 24 hour records could be implemented. Analysis of activity in multiple muscles during clonus may reveal the overall behavior of the limb. This study demonstrated the potential usefulness of analyzing long term recordings to understand the nature of clonus and its prevalence. The algorithm could also be a prospective diagnostic tool to characterize clonus to judge the effectiveness of interventions like drugs that are used to mitigate clonus.

Chapter 7: Conclusions

The algorithm developed in this study using MATLAB aimed to automatically detect the start and end times of EMG bursts during clonus recorded from leg muscles paralyzed by SCI. The program was highly reliable and as accurate as two independent raters in identifying EMG bursts, measuring the duration of EMG bursts, clonus frequency, and the intensity of contractions. The algorithm was also significantly faster than people at measuring the start and end times of EMG during clonus.

The novel methods developed in this study were used to analyze EMG recorded from medial gastrocnemius over 24 hours from one subject who had a spinal cord injury at C4. This analysis showed that clonus was more common during awake time than during sleep. Clonus during awake hours also had much stronger contractions than those during sleep time.

In terms of potential applications of the algorithm, it may be useful to characterize clonus and its behavior across an entire day. The data gathered can answer questions about the prevalence of clonus after SCI and whether it can be dampened by medication, exercise or other interventions.

References

- Adams MM & Hicks AL (2005). Spasticity after spinal cord injury. *Spinal Cord* 43, 577-586.
- Beres-Jones JA, Johnson TD, & Harkema SJ (2003). Clonus after human spinal cord injury cannot be attributed solely to recurrent muscle-tendon stretch. *Exp Brain Res* 149, 222-236.
- Cook WA, Jr. (1967). Antagonistic muscles in the production of clonus in man. *Neurology*, 779-796.
- Dietz V, Trippel M, & Berger W (1991). Reflex activity and muscle tone during elbow movements in patients with spastic paresis. *Ann Neurol* 30, 767-779.
- Dimitrijevic MR, Nathan PW, & Sherwood AM (1980). Clonus: the role of central mechanisms. *J Neurol Neurosurg Psychiatry* 43, 321-332.
- Ellingson Amanda Jo. Leg muscles. Available at: <http://www.amandajoellingson.com>. Accessed February 6, 2009.
- Gerrits HL, De HA, Hopman MT, van Der Woude LH, Jones DA, & Sargeant AJ (1999). Contractile properties of the quadriceps muscle in individuals with spinal cord injury. *Muscle Nerve* 22, 1249-1256.
- Grimby G, Broberg C, Krotkiewska I, & Krotkiewski M (1976). Muscle fiber composition in patients with traumatic cord lesion. *Scand J Rehabil Med* 8, 37-42.
- Häger-Ross CK, Klein CS, & Thomas CK (2006). Twitch and tetanic properties of human thenar motor units paralyzed by chronic spinal cord injury. *J Neurophysiol* 96, 165-174.
- Hidler JM & Rymer WZ (2000). Limit cycle behavior in spasticity: analysis and evaluation. *IEEE Trans Biomed Eng* 47, 1565-1575.

- Ianssek R (1984). The effects of reflex path length on clonus frequency in spastic muscles. *J Neurol Neurosurg Psychiatry* 47, 1122-1124.
- Klein CS, Häger-Ross CK, & Thomas CK (2006). Fatigue properties of human thenar motor units paralysed by chronic spinal cord injury. *J Physiol* 573, 161-171.
- Lance JW (1980). Symposium synopsis. In *Spasticity: Disordered Motor Control*, eds. Feldman RG, Young RR, & Koella WP, pp. 485-494. Year Book Medical, Chicago, III.
- Lin JP, Brown JK, & Walsh EG (1999). Continuum of reflex excitability in hemiplegia: influence of muscle length and muscular transformation after heel-cord lengthening and immobilization on the pathophysiology of spasticity and clonus. *Dev Med Child Neurol* 41, 534-548.
- Maynard FM, Jr., Bracken MB, Creasey G, Ditunno JF, Jr., Donovan WH, Ducker TB, Garber SL, Marino RJ, Stover SL, Tator CH, Waters RL, Wilberger JE, & Young W (1997). International Standards for Neurological and Functional Classification of Spinal Cord Injury. American Spinal Injury Association. *Spinal Cord* 35, 266-274.
- Mogenson, Gordon J (1977), *Nerve cells and Behavior Part I*, pp. 25. L.Eribaum Associates, New Jersey.
- Nunnally JC & Bernstein IH (1994). *Psychometric theory*, 3rd edition ed., pp. 83-113. McGraw-Hill, New York.
- Rack PM, Ross HF, & Thilmann AF (1984). The ankle stretch reflexes in normal and spastic subjects. The response to sinusoidal movement. *Brain* 107, 637-654.
- Rossi A, Mazzocchio R, & Scarpini C (1990). Clonus in man: a rhythmic oscillation maintained by a reflex mechanism. *Electroencephalogr Clin Neurophysiol* 75, 56-63.
- Sheean G (2002). The pathophysiology of spasticity. *European Journal of Neurology* 9, S3-S9.

- Shields RK (1995). Fatigability, relaxation properties, and electromyographic responses of the human paralyzed soleus muscle. *J Neurophysiol* 73, 2195-2206.
- Shields RK (2002). Muscular, skeletal, and neural adaptations following spinal cord injury. *J Orthop Sports Phys Ther* 32, 65-74.
- Shrout PE & Fleiss JL (1979). Intraclass correlation: uses in assessing rater reliability. *Psychol Bull* 86, 420-428.
- Thomas CK (1997). Contractile properties of human thenar muscles paralyzed by spinal cord injury. *Muscle Nerve* 20, 788-799.
- Thomas CK, Johansson RS, & Bigland-Ritchie B (2006). EMG changes in human thenar motor units with force potentiation and fatigue. *J Neurophysiol* 95, 1518-1526.
- Thomas CK & Zijdwind I (2006). Fatigue of muscles weakened by death of motoneurons. *Muscle Nerve* 33, 21-41.
- Von Tscharner, V (2000). Intensity analysis in time-frequency space of surface myoelectric signals by wavelets of specified resolution. *J Electromyogr Kinesiol* 10, 433-445.
- Von Tscharner, V (2002). Time-frequency and principal-component methods for the analysis of EMGs recorded during a mildly fatiguing exercise on a cycle ergometer. *J Electromyogr Kinesiol* 12, 479-492.
- Von Tscharner, V, Goepfert B, & Nigg BM (2003). Changes in EMG signals for the muscle tibialis anterior while running barefoot or with shoes resolved by non-linearly scaled wavelets. *J Biomech* 36, 1169-1176.
- Wallace DM, Ross BH, & Thomas CK (2005). Motor unit behavior during clonus. *J Appl Physiol* 99, 2166-2172.
- Walsh EG (1976). Clonus: beats provoked by the application of a rhythmic force. *J Neurol Neurosurg Psychiatry* 39, 266-274.